Blackwell
Publishing Asia

GUIDELINES FOR THE USE OF PDF VERSIONS OF ARTICLES

Dear Author

You have been sent a portable document format file ('PDF offprint') containing the final version your paper that was recently published in our Journal. Please note that use of this PDF is governed by the following guidelines.

1. The Corresponding Author of the article may, without charge, photocopy or transmit online or download, print out and distribute to co-authors and colleagues this PDF file of the published article, in whole or in part, for the Corresponding Author's personal or professional use, for the advancement of scholarly or scientific research or study.

2. This PDF file may be posted on the Corresponding Author's own website for personal or professional use or on the Corresponding Author's internal university or corporate network/intranet, or on a secure, closed section of an external website at the Corresponding Author's institution. The Abstract may be posted on a public access section of any website.

3. If this PDF file is posted on a website, the Corresponding Author must ensure that it is accompanied by a notice that states the full details of the article (journal title, year of publication, volume and page numbers that the article appears on) and its availability on Blackwell *Synergy*. Please use the example below as a template for presenting your article's details:

   > This article was published in *Journal of Statistical Methods in Research Science*, 2004; 3: 189–200, available online at Blackwell *Synergy* (www.blackwell-synergy.com).

   Please ensure the Blackwell *Synergy* URL appears as a live link.

4. This PDF file may not be offered for commercial sale or for any systematic external distribution by a third party (e.g. a listserve or database connected to a public access server).

5. The Corresponding Author agrees not to update or change this PDF file.

If you have any queries regarding the use of this PDF file, please contact info@blackwellpublishingasia.com.

Blackwell Publishing Asia Pty Ltd
ACN004901562
ABN 29004901562

Melbourne office
550 Swanston Street
PO Box 378
Carlton South
Victoria 3053
Australia

Tel: +61 3 8359 1011
Fax: +61 3 8359 1120
info@blackwellpublishingasia.com

Available online at www.sciencedirect.com
SCIENCE DIRECT
Biochemical Pharmacology 69 (2005) 503–516
Biochemical Pharmacology
www.elsevier.com/locate/biochempharm

Some flavonoids and DHEA-S prevent the *cis*-effect of expanded CTG repeats in a stable PC12 cell transformant

Hirokazu Furuya[a,b,*], Nobue Shinnoh[a], Yasumasa Ohyagi[a], Koji Ikezoe[a], Hitoshi Kikuchi[a], Manabu Osoegawa[a], Yasuyuki Fukumaki[c], Yusaku Nakabeppu[d], Toshimitsu Hayashi[e], Jun-ichi Kira[a]

[a]*Department of Neurology, Neurological Institute, Graduate School of Medical Sciences, Kyushu University, Fukuoka 812-8582, Japan*
[b]*Department of Neurology, National Omuta Hospital, Fukuoka, 837-0911, Japan*
[c]*Division of Disease Genes, Research Center for Genetic Information, Medical Institute of Bioregulation, Kyushu University and CREST, JST, Fukuoka 812-8582, Japan*
[d]*Division of Neurofunctional Genomics, Medical Institute of Bioregulation, Kyushu University and CREST, JST, Fukuoka 812-8582, Japan*
[e]*Faculty of Pharmaceutical Sciences, Toyama Medical and Pharmaceutical University, 2630 Sugitani, Toyama 930-0194, Japan*

Received 9 July 2004; accepted 20 October 2004

Abstract

Expanded CUG triplet repeats carrying mRNA seem to be responsible for myotonic dystrophy type 1 (DM1). To study the pathogenesis of DM1, we constructed a DM1 cell culture model using a PC12 neuronal cell line and screened flavonoids that ameliorate this mRNA gain of function. The expanded 250 CTG repeat was subcloned into the 3′-untranslated region of the luciferase gene yielding a stable transformant of PC12 (CTG-250). The cytotoxicity of CTG-250 was evaluated by intracellular LDH activity, and the *cis*-effect by luciferase activity. To find agents that alter CTG-250 toxic effects, 235 bioflavonoids were screened. An increased *cis*-effect and cytotoxicity were found when CTG-250 was treated with nerve growth factor to induce differentiation. Western blotting with anti-caspase-3 antibody suggested that cell death was caused by apoptosis. Screening analysis confirmed that a flavone (toringin), an isoflavones (genistein and formononetin), a flavanone (isosakuranetin), and DHEA-S prevent both the cytotoxicity and *cis*-effect of CTG-250 and that a flavanone (naringenin), isoflavone (ononin), and xanthylatin strongly inhibit the *cis*-effect of CTG repeats. In conclusion, we found that this neuronal cell line, which expresses the CUG repeat-bearing mRNA, showed *cis*-effects through the reporter gene and neuronal death after cell differentiation in vitro. However, some flavonoids and DHEA-S inhibit both the *cis*-effect and cytotoxicity, indicating that their chemical structures work to ameliorate both these toxic effects. This system makes it easy to evaluate the toxic effects of expanded CTG repeats and therefore should be useful for screening other DM1 treatments for their efficacies.

Keywords: Myotonic dystrophy type 1; Trinucleotide repeats; PC12; Flavonoid; RNA gain of function; Tauopathy

1. Introduction

Myotonic dystrophy, type 1 [MIM 160900; dystrophia myotonica 1 (DM1)] is an autosomal dominant form of muscular dystrophy. Although its common features are myotonia and progressive type 1 dominant muscle fiber atrophy, other frequent defects are cardiopathy, cataracts, insulin resistance, frontal balding, mild dementia, and other systemic involvements [1]. To date, two mutations (DM1 and DM2 [MIM 602668; dystrophia myotonica 2 (DM2)]), at unlinked loci, are known to be associated with myotonic dystrophy.

The DM1 mutation has been identified as an expanded CTG trinucleotide repeat tract in the 3′-untranslated region (3′-UTR) of the DM1 protein kinase (DMPK) gene [2]. In DM1 patients, the mRNA for DM1 protein kinase (*DMPK*)

Abbreviations: DM1, myotonic dystrophy type1; DM2, myotonic dystrophy type2; DMPK, DM1 protein kinase; 3′-UTR, 3′-untranslated region; RT-PCR, reverse transcription polymerase chain reaction; MW, molecular weight; kDa, kilo-Dalton; EtBr, ethidium bromide; conc., concentration; nt, nucleotides length; DHEA-S, dehydroepiandrosterone sulfate; DMSO, dimethyl sulfoxide; DMEM, Dulbecco's modified Eagle's medium; CNS, central nervous system

* Corresponding author. Tel.: +81 92 642 5340; fax: +81 92 642 5352.
E-mail address: furuya@neuro.med.kyushu-u.ac.jp (H. Furuya).

0006-2952/$ – see front matter © 2004 Elsevier Inc. All rights reserved.
doi:10.1016/j.bcp.2004.10.005

has from 50 to more than 2000 CTG repeats in its 3′-untranslated region (3′-UTR) [3]. Although this DM1 mutation accounts for 98% of DM cases, it is not known exactly how it causes the disease [4]. Several mechanisms, which indicate altered DMPK and/or isoforms, and mis-expression of self or neighboring genes at the DM1 locus (*cis*-effect), and/or at *trans*-dominant mutant DMPK mRNA (*trans*-effect), have been proposed [5].

Recently, a CCTG repeat expansion disease (DM2), in which the CCTG repeat is in intron 1 of the *zinc finger protein 9* (*ZNF9*) gene, has been reported [6,7]. Like the CUG-bearing RNA in DM1, the CCUG-bearing RNA in DM2 accumulates at a small number of foci in the nucleus. The expression of RNA carrying either a CUG or CCUG expanded repeat, rather than a deficiency of the DMPK, SIX5 or ZNF9 proteins, therefore is thought to account for the disease features common to DM1 and DM2 [4]. Mutant transcripts are retained in the nuclei of mouse C2C12 myoblast cells and aggregate into distinct foci [8,9]. Moreover, there is increasing evidence that mutant DMPK mRNA acts in *trans*- to disrupt cellular RNA metabolism (the toxic RNA theory of DM1 or RNA gain of function theory) [10-12]. Further, we have shown that CTG repeats interfere with the expression of the reporter gene in *Xenopus* oocytes but not in embryos (fertilized eggs). Early embryonic cells undergo extensive division, whereas the oocyte nucleus never divides and does not liberate nuclear materials into the cytoplasm. CTG repeats therefore are thought to interfere with the nucleus–cytoplasm transport of mRNA, especially at the nuclear membrane, rather than transcription of the gene [13].

To explain how RNA gain of function causes DM1, the protein sequestration hypothesis has been proposed [10-12,14]. According to this hypothesis, the DM1 expansion leads to sequestration of $(CUG)_n$ binding proteins on mutant DMPK RNAs and depletion from other transcripts that require these proteins for normal gene expression. Several $(CUG)_n$ binding proteins have been subcloned, and proteins in the MBNL(muscleblind-like) family bind to expanded CUG repeats in vitro and colocalize with mutant DM transcripts in vivo [11,15,16]. Expression of CUG and CCUG expansion RNAs induces MBNL recruitment into nuclear RNA foci, and disruption of the mouse Mbnl1 gene leads to muscle, eye, central nervous system (CNS) and RNA splicing abnormalities that are characteristic of DM1 [11,17,18].

The human CNS has tau proteins that consist of six isoforms which differ by the presence or absence of alternatively spliced exons 2, 3 and 10. The main pattern of aggregated tau isoforms in DM1 brain lesions is the shortest human tau isoform. Reduced expression of tau isoforms containing exon 2 occurs at both the mRNA and protein levels [19]. The same tau isoform pattern occurs in the CNS of a mouse transgenic model for DM1 [20]. These findings indicate that normal neuronal functions are disturbed by the CTG repeat expansions, resulting in abnormal phosphorylation of tau protein, which has recently been called tauopathy. Further, the expanded CTG_{90} repeats is reported to inhibit neuronal differentiation in a PC12 rat neuronal cell line [21].

We established a PC12 cell line that stably expresses expanded 250 CUG repeat-bearing mRNA. In this system, mitosis occurs, and the nuclear membrane disappears during every mitotic period until cell differentiation starts, but once differentiation starts, mitosis never occurs [22]. We hypothesized that this system shows the toxicity of CUG repeat-expanded mRNA after cell differentiation much more effectively than do cell lines with frequent mitosis. Since tau plays a significant role in the cytoskeletal changes that occur during apoptosis in the PC12 cell line [23], for example, in the histopathology of Alzheimer's disease patients or tauopathy, and because the removal of serum from the culture medium causes oxidative stress and triggers cell injury characterized by signs of apoptosis [24,25], we first examined the abnormal phosphorylation of tau protein resulting from the different alternative splicings of the tau gene using this system. We confirmed the cytotoxicity and *cis*-effect of the expanded repeat under the oxidative stress after neuronal cell differentiation in vitro.

Then, we screened chemicals that ameliorate the cytotoxicity and *cis*-effect of toxic RNA with expanded CUG repeats. For the screening, panels of bio-flavonoids were the candidates for treatment because (1) flavonoids are ubiquitous polyphenolic compounds in the human diet, (2) the basic flavonoid structure is very simple, but there are hundreds of derivatives, and (3) some flavonoids have a variety of biological activities that include beneficial effects on cancer or for coronary heart disease prevention [26]. We found that some bioflavonoids inhibit the cytotoxicity and/or *cis*-effect of expanded CTG repeats carrying mRNA.

2. Materials and methods

2.1. Plasmid constructions

A CTG repeat-bearing DNA fragment was isolated from genomic DNA extracted from leukocytes obtained from a mildly affected 47-year-old male with DM1 after obtaining his informed consent. When this genomic DNA was subjected to Southern blot analysis, it was found to carry a 250 CTG repeat expansion. The amplified DNA fragment with the repeats was digested with *Msp*I and subcloned into the luciferase expression vector pGL3 (Promega) at the blunt-ended *Xba*I sites. The pGL3 vector carrying the luciferase gene and 250 CTG repeats was digested with *Hin*dIII and *Bam*HI, blunt-ended and then subcloned into the *p*CAGGS*neo* vector [27] at the blunt-ended *Eco*RI site. Subcloned plasmids were sequenced by the dideoxy sequencing method with a Dye Deoxy Terminator Kit (Perkin-Elmer Applied Biosystems).

2.2. Cell culture and transfection

PC12 cells were maintained as described elsewhere [28]. Cells plated on collagen-coated dishes (Sigma) were transfected with reporter plasmids by means of the Lipofectamin Plus Reagent (Gibco-BRL). Stable transfectants were isolated after extended culture in growth medium containing 0.4 mg/ml Neomycin (Gibco-BRL). Surviving cells were re-cultured, and luciferase activity was measured to screen for colonies with a high level of expression. A RT-PCR done on the mRNA extracted from these stable cells was performed to analyze whether the clones had 250 CTG repeats. A selected PC12 cell line carrying 250 CTG repeats and efficiently expressing the luciferase gene was named CTG-250. A cell line that expresses the luciferase reporter gene only was named LUC and used as the control. To induce differentiation, cells were treated with 100 ng/ml nerve growth factor (NGF; Gibco-BRL) for up to 7 days. Serum was removed by replating the differentiated PC12 cells onto new collagen-coated dishes as described elsewhere [29], and cells were maintained in 100 ng/ml NGF with serum-free medium for the appropriate period under oxidative stress [24,25]. For immunohistochemical analysis, cells were reseeded onto glass coverslips in 24-well plates coated with 12 μg/ml poly D-lysine (Sigma).

2.3. Immune fluorescence microscopy

For immuno-histochemical analysis, cells were reseeded onto glass coverslips in 24-well plates coated with 12 μg/ml poly D-lysine (Sigma) at a density of 2.5×10^4 cells/well. Two to 6 days after reseeding with NGF in serum-free medium, cultured the PC12 cells placed cultured on coverslips were fixed with 4% paraformaldehyde-phosphate-buffered saline (PBS) for 15 min. After residual formaldehyde had been quenched with 50 mM NH4Cl-PBS for 10 min, cells were permeabilized in 0.2% Triton X-100-PBS for 10 min and incubated with 10% fetal bovine serum in PBS for 30 min to block nonspecific antibody binding. Cytoplasmic neurofilaments were detected with an anti-neurofilament 200 kDa monoclonal antibody (clone NE14, Boehringer Mannheim Biochemica) in PBS (0.5 U/ml) for 1 h. Cells on coverslips were mounted in 90% glycerol containing 0.1% *p*-phenylenediamine dihydrochloride in PBS and examined by the method described elsewhere (Fig. 1c) [30]. All the steps were done at room temperature, and the cells were rinsed with PBS between steps.

2.4. RNA extraction and reverse transcription

Total RNA was extracted from the cultured cells with RNeasy Mini (Qiagen), and the concentration measured by means of a NanoDrop (NanoDrop Tech) then used for Northern blotting and the RT-PCR. One microgram of total RNA was reverse transcribed with a First-Strand cDNA

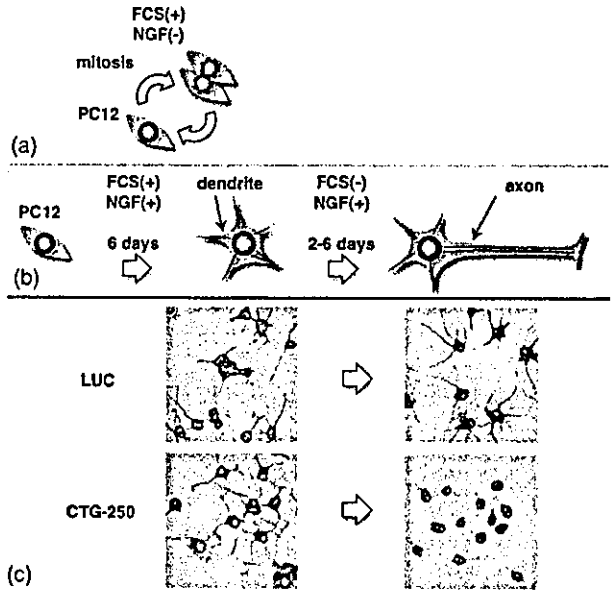

Fig. 1. Schematic presentation of the PC12 cell cycle without differentiation (a), with differentiation (b), and the effect of CTG repeat expression on neurite outgrowth in NGF-treated stably transfected PC12 cell lines under oxidative stress (c). Immunohistochemical staining of the LUC control and CTG-250 neuronal cell lines is shown (neurofilament (NF) staining, 200×). Photos of cells are placed under the corresponding cell figure (c). The nuclear membrane of PC12 cells disappears during every mitotic event (broken line) (a). After cellular differentiation by NGF during 6 days of incubation with fetal calf serum (FCS), PC12 cell mitosis stops, the nuclear membrane is maintained and dendrites and axons are formed (FCS(+), NGF(+)) (b). Note deterioration of the axon and dendrite processes in CTG-250 cells cultured without FCS, but with NGF (FCS(−), NGF(+)) for 2–6 days (c).

Synthesis Kit (Pharmacia Biotech) using random hexamers. After incubation, the reaction mixture was diluted to 30 μl with water, and 1 μl of the dilution was used for the RT-PCR analysis.

2.5. Northern blot hybridization

Five micrograms of the total RNA from each cell was electrophoresed in an agarose gel and then transferred to a Hybond N^+ membrane (Amersham Inc.). These membranes were hybridized with a ^{32}P-labeled luciferase cDNA probe, labeled by the Random Primer labeling system using [^{32}P]dCTP as the radioactive nucleotide. Blots were exposed on imaging plates, and the radioactivity of the bands quantified with the BAS2000 System (Fuji film Inc.). The radioactivity of the mRNA bands from each cultured cell obtained at each time point (24–48 h) was calculated as the ratio of the value obtained for the undifferentiated CTG-250 cell line. Hybridized blot analysis was performed three times (Fig. 2).

2.6. RT-PCR

PCR amplification of the tau transcripts was done with rat tau primers that recognize differences in the sizes of tau gene products. No DNA amplification was found in the

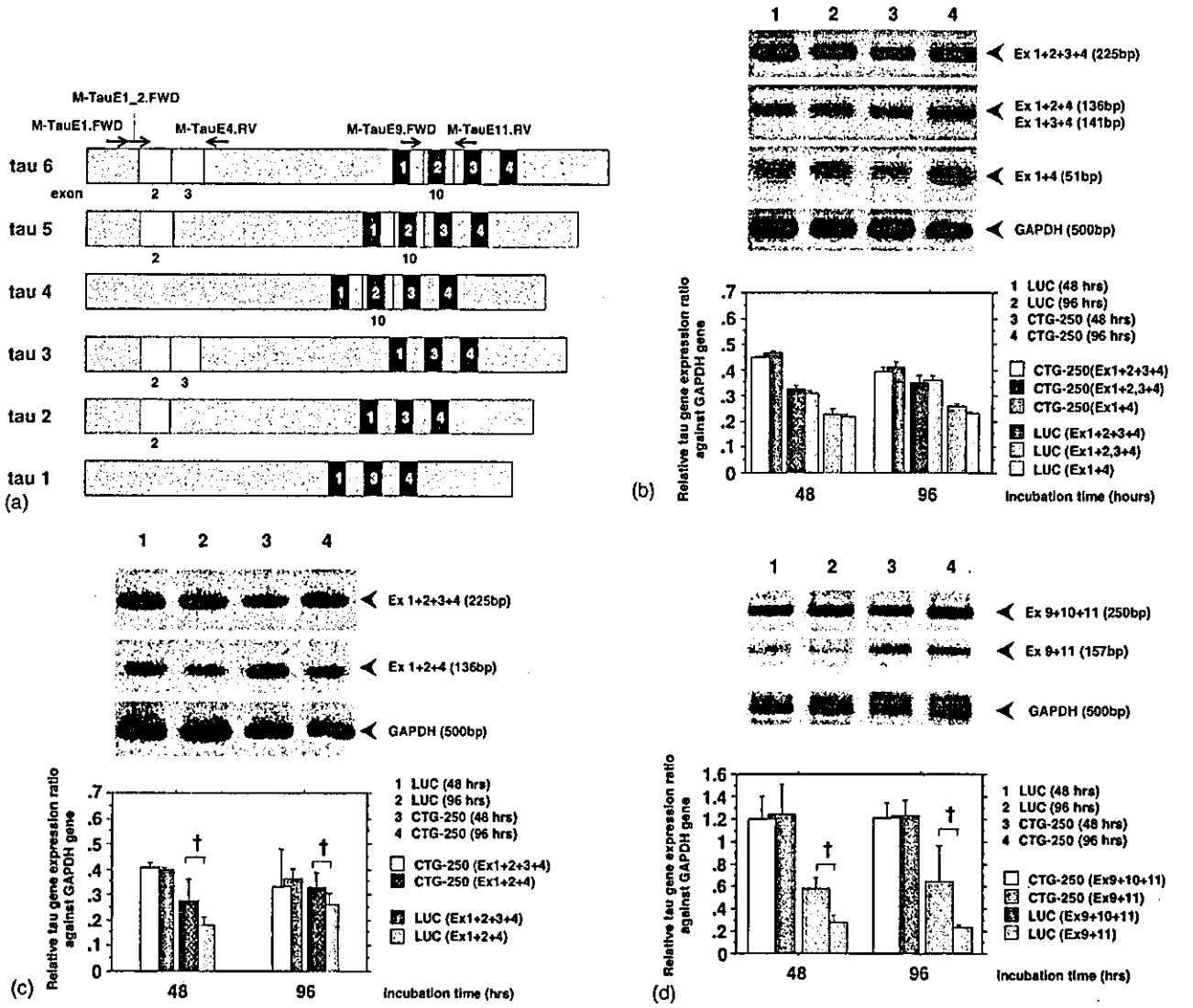

Fig. 3. (a) Diagram of tau isoform structures [34]. Alternatively spliced exons are shown as white boxes. Regions common to all isoforms are shaded. Microtubule (MT) binding repeats (three or four) are indicated as numbered black boxes. The diagram is not drawn to scale. Names and locations of the primers used for the RT-PCR are shown as relative positions at the top. The six tau isoforms, taus 1–6, were derived by alternative splicing of exons 2, 3, and 10, three with and three without exon 10, that encode for the additional MT-binding repeat. (b) Expression profile of rat tau mRNA isoforms. RT-PCR products corresponding to the various isoforms were obtained with two sets of primers. Primers M-tauE1.FWD and M-tauE4.RV (b) or M-tauE1_2.FWD and M-tauE4.RV (c) were also used to differentiate tau mRNA isoforms that have or lack exons 2, 3 or both (a). Tau mRNA isoforms, that have or lack exon 10 also were identified with primers M-TauE9.FWD and M-TauE11.RV (d). LUC control cells after 48 h (lane 1), and 96 h (lane 2) incubations with differentiation; CTG-250 cells after 48 h (lane 3), 96 h (lane 4) incubations with differentiation (b–d). GAPDH was the internal standard. Relative tau expression ratios are shown in the lower berth of each figure. Data are expressed as transcribed tau gene products normalized to GAPDH gene expression, mean ± S.E.M. ($n = 3$ in separate experiments). $^{\dagger}P < 0.05$ compared with PC12 cells without expanded CTG repeats (LUC). Note the decrease in tau mRNA isoforms that lack exons 3 and 10 after differentiation for 48–96 h.

Chemiluminescence System (ECL system) (Amersham Pharmacia Biotech).

2.9. *Luciferase assay and LDH cytotoxicity detection assay*

To evaluate the transcription and translation of the CTG repeat-bearing reporter gene, luciferase activity was assayed with a Luciferase Assay System according to the manufacturer's protocol (Promega Co.). After CTG-250 and LUC cell differentiation with NGF, PC12 cells were plated in 96-well plates at 1.3 × 104 cells/well. After 2–6 days incubation period with a flavonoid under oxidative stress, the cells were washed with PBS and assayed (Figs. 4a, 6a, 7a, 8a, and 9a). The amount of protein in each sample was determined by the Lowry–Folin assay [32]. Luciferase activity was expressed on a per-protein basis.

To determine the cytotoxic effect of the expanded CTG repeat, lactate dehydrogenase (LDH) activity in the cell was measured as a gauge of the total number of living cells with a kit from Takara (LDH Cytotoxicity Detection Kit).

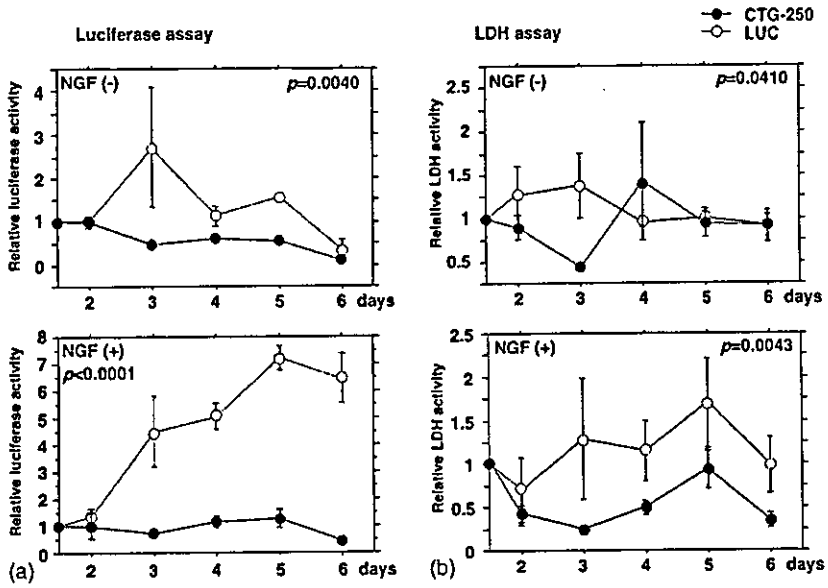

Fig. 4. In vitro luciferase (a) and LDH (b) assay of cultures without (upper graphs) and with (lower graphs) NGF and the incubation periods. The graphed points represent the means ± standard errors of the LUC (○) and CTG-250 (●) cells. Values shown are ratios to luciferase or LDH activity without incubation. Note that the luciferase activity of LUC cells with NGF is significantly increased ($P < 0.0001$) vs. that of CTG-250 cells. as incubation progresses. The LDH activity of CTG-250 decreased slightly ($P = 0.0043$) when incubated with NGF.

Results are shown as intracellular LDH activity on a per-protein basis (Figs. 4b, 6b, 7b, 8b and 9b).

2.10. First screening of bioflavonoids and other chemicals for RNA gain of function prevention

In the cell treatment experiment, 235 purified bioflavonoids and other chemicals that structurally resemble bioflavonoids were screened initially. All bioflavonoids were supplied from by the Laboratory of Pharmacognosy, Toyama Medical and Pharmaceutical University. They were originally obtained by isolation from higher plants growing in Japan. Most of them were identified by spectral analyses. Some compounds were obtained by chemical modification of the isolated compounds. The purity of each compound was checked by thin layer chromatography, NMR spectrum, and elemental analysis. The bioflavonoids and other chemicals were dissolved in dimethyl sulfoxide (DMSO) at a maximum DMSO concentration of 0.5%. After differentiation, PC12 cells (LUC and CTG-250) were re-plated in collagen-coated 96-well plates at 1.3 × 104 cells/well in serum-free medium containing 100 ng/ml NGF and 10 μg/ml of each flavonoid for cell treatment. After 2 days of incubation, the cells were washed with PBS, lysed in Cell Lysate Buffer (Promega Co.), and used in the luciferase assay. Luciferase activity data were compared with the data for untreated cells. Flavonoids and other related chemicals that produced luciferase activity more than three times that of the untreated controls were selected and prepared for second and third screenings. DHEA-S was used for in the second screening directly because its effectiveness has already reported [33].

2.11. Second and third screenings of flavonoids and other chemicals

After differentiation, PC12 cells (LUC and CTG-250) were re-plated in collagen-coated 96-well plates at 1.3 × 104 cells/well in serum-free medium containing 100 ng/ml NGF. Various concentrations of flavonoids for cell treatment (10, 20, 40, and 80 μg/ml in the second screening, and 5, 10, 20, 80, and 160 μg/ml in the third) were added on the second and fourth days of culture. Luciferase activities of the CTG-250 and LUC cell lines were compared over the time course. Several flavonoids and other chemicals had statistically significant effectiveness in preventing the *cis*-effect, cytotoxicity of expanded CTG repeats or both (Figs. 6–9 and Table 1). The chemical structures of those flavonoids are presented in Fig. 5.

2.12. Data analysis and statistics

The expression of the luciferase gene in Northern blotting and of the tau protein in RT-PCR were determined by use of the National Institutes of Health Image-J (V1.31b), Java-based image processing program in a Macintosh OS X based computer system. Data were analyzed statistically by the Student's *t*-test and repeated measures ANOVA.

Data obtained from the experiment that detected RNA gain of function with or without differentiation were expressed as ratios of their respective control values obtained on the first day of sample re-plating, which was not under differentiated conditions (FCS(+), NGF(−), in Fig. 1a) (Fig. 4). In the cell treatment experiment with bioflavonoids and other chemicals, the data are expressed as ratios of the respective control values for the untreated

Table 1
Inhibitory effect of flavonoids on expanded 250 CTG repeats transcribing PC12 neuronal cell (CTG-250)

Chemical name (MW)	Conc. (μg/μl)	Conc. (μM)	*Cis*-effect	Cytotoxicity
Flavone				
Baicalein (280)	5	17.9	+	–
	10	35.7	+	–
	20	71.4	+	–
Toringin (416)	5	12.0	–	–
	10	24.0	–	–
	20	48.0	+	+
Cosmosiin (432)	5	11.6	–	–
	10	23.1	–	–
	20	46.3	–	–
Acacetin (284)	5	17.6	–	–
	10	35.2	–	–
	20	70.4	–	–
Apigenin (270)	5	18.5	+	–
	10	37.0	+	–
	20	74.0	+	–
Irisolone (312)	5	16.0	+	–
	10	32.0	–	–
	20	64.1	–	–
Genkwanin (284)	5	17.6	+	–
	10	35.2	+	–
	20	70.4	–	–
Isoflavone				
Genistein (270)	5	18.5	–	–
	10	37.0	+	+
	20	74.0	–	–
Formononetin (268)	5	18.7	++	–
	10	37.3	++	–
	20	74.6	–	–
Ononin (430)	5	11.6	++	–
	10	23.2	+	–
	20	46.5	–	–
Daidzein (254)	5	19.7	–	–
	10	39.4	–	–
	20	78.7	–	–
Flavanone				
Isosakuranetin (286)	5	17.4	–	–
	10	34.9	+	–
	20	69.9	++	++
Naringenin (272)	5	18.4	–	–
	10	36.8	+	–
	20	73.5	++	–
Coumarin				
Xanthylatin (228)	5	21.9	–	–
	10	43.9	++	–
	20	87.7	++	–
Steroid				
DHEA-S (368)	5	13.6	+	–
	10	27.2	+	+
	20	54.3	–	–

(+) effective for inhibition ($P < 0.05$); (++) highly effective for inhibition ($P < 0.0001$); (–) not effective for inhibition; MW, molecular weight; DHEA-S, dehydroepiandrosterone-sulfate.

cells (FCS(–), NGF(+), Fig. 1b) (Figs. 6–9). Data are expressed as means ± S.D. A repeated measures ANOVA was used for the statistical analysis between CTG-250 and LUC cells based on the time courses in all the experiments related to detecting *cis*-effect and cytotoxicity (Figs. 4 and 6–9, Table 1). Three separate experiments were performed. A P value <0.05 was considered significant.

The results of in vitro luciferase and LDH assay cultures without and with NGF were analyzed according to the time course (Fig. 4). Thus, the result is displayed only as a P value. The data on inhibition of the *cis*-effect and cytotoxicity by bioflavonoids (Figs. 6–9) was analyzed with ANOVA according to the time course (two and four incubation days) between CTG-250 and LUC cells, and the results are shown in the graph at various bioflavonoid concentrations (0, 5, 10 and 20 μg/ml). Thus, the results of statistical analyses are shown by symbols on the graph.

3. Results

3.1. Establishment of stable PC12 clones

Luciferase was used as the reporter gene to determine the *cis*-effect of the CUG repeat expansion in the 3′-UTR region of the RNA. Reporter plasmids that carried the 3′-UTR region, with or without expanded CTG repeats, were transfected into PC12 cells, producing several stable clones that were selected by the neomycin resistance of each construct. PC12 cells have been widely used as a model for studying the characteristics of neuronal cells because they respond to NGF and differentiate into cells that are morphologically and biologically similar to neurons (Fig. 1a and b). A PCR done on the genomic DNA extracted from these stable cells, performed to analyze whether the clones had CTG repeats in their genomes and expressed CUG repeats carrying RNA in vitro, confirmed the presence of the expanded CTG repeat (data not shown). Northern blotting with luciferase cDNA as the probe also showed expanded 250 CUG repeats and the same luciferase mRNA intensities in CTG-250 and LUC, evidence of the successful transcription of the luciferase gene in this system (Fig. 2).

3.2. mRNA carrying expanded CUG repeats produce different patterns of alternative splicing of the tau gene but not abnormal phosphorylation

Because differences in the alternative splicing of the tau gene and the abnormal phosphorylation of tau protein have been reported in brains of DM1 patients and in a DM1 mouse model [19,20,34], we examined splicing and phosphorylation in our PC12-based cell system. When primer sets detecting tau1-6 isoforms (M-TauE1.FWD and M-TauE4.RV) (Fig. 3a) were used, no difference in the expression patterns of tau isoforms was detected (Fig. 3b). However, when a primer set that specifically encodes tau 2, 3, 5, 6 were used (M-TauE1_2.FWD and M-TauE4.RV) (Fig. 3a), decreased expression of the exon 3 spliced-out isoform was confirmed (Fig. 3c). These results indicate that in the CTG-250 PC12 cell line, tau 2 or tau 5 isoforms, rather than tau 3 or tau 6 isoforms, are increased.

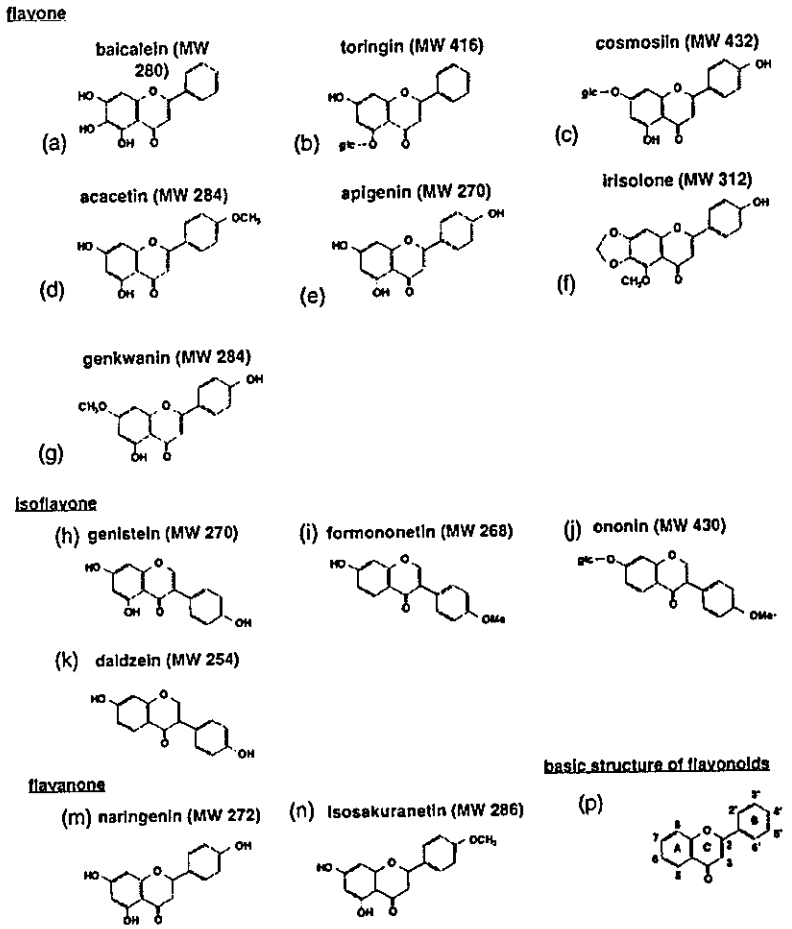

Fig. 5. Structures of flavonoids and the other test chemicals of (1) the flavone family, (2) the isoflavone, flavanone family and the basic structure of flavonoids, MW: molecular weight.

These findings are compatible with previous reports [19,20], but there is a different tau isoform expression pattern, a splice out of exon 10 of the tau gene, also was present in our CTG-250 cell line (Fig. 3d). A different abnormal phosphorylation pattern also has been reported in DM1 patients and in the DM1 mouse model [19,20], but no significant difference in the phosphorylation pattern was found for the stable, repeat-expressing PC12

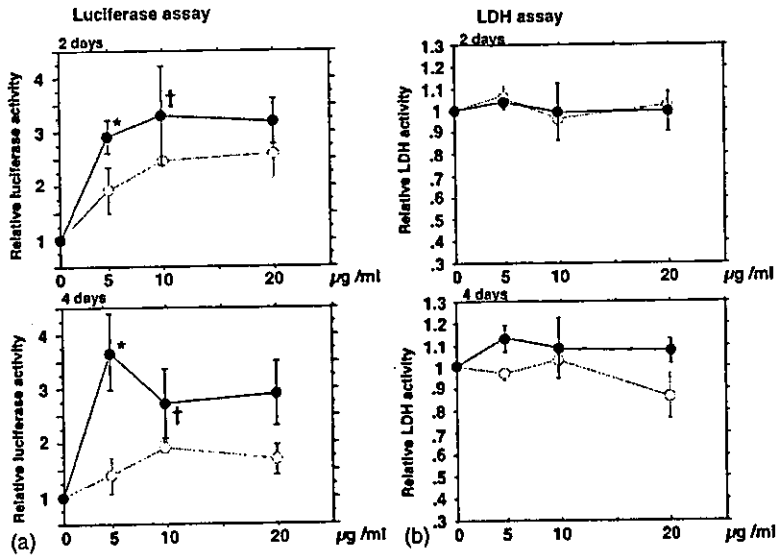

Fig. 6. Inhibition by ononin (isoflavone) of the *cis*-effect (a) and cytotoxicity (b) caused by expanded CTG repeats. The points represent means ± standard errors of LUC (○) and CTG-250 (●) cells. Values are ratios for luciferase (a) or LDH activity (b) for each untreated cell. The upper boxes shown findings after 2 days of incubation, the lower ones after 4 days of incubation (FCS(−), NGF(+)). Statistical significance also is shown ($^{*}P < 0.0001$; $^{\dagger}P < 0.05$).

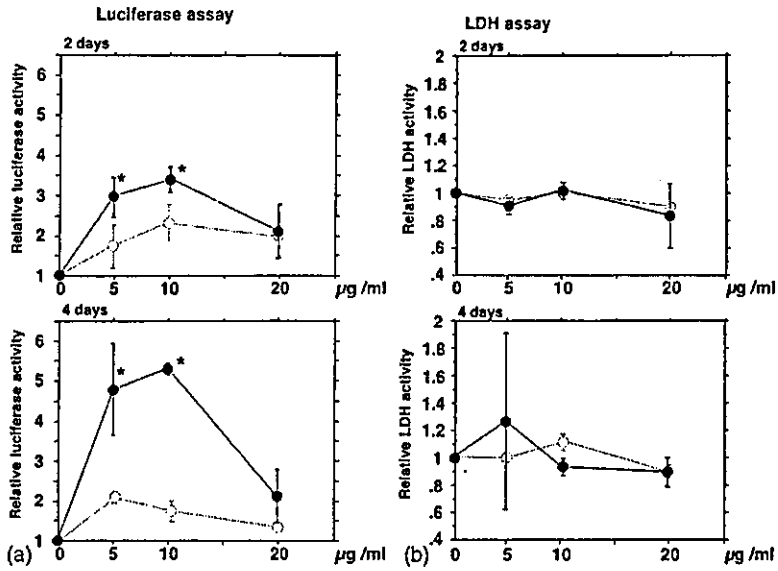

Fig. 7. Inhibition by formononetin (isoflavone) of the *cis*-effect (a) and cytotoxicity (b) caused by expanded CTG repeats (data and abbreviations are the same as in Fig. 6).

(CTG-250) and control cell lines (LUC) (data not shown).

3.3. mRNA carrying expanded CUG repeats shows cytotoxicity

To investigate the effect of expanded CTG repeat transcription on the neuronal differentiation and cytotoxicity of PC12 cells, morphological changes in the stable clones were examined during NGF-induced differentiation (Fig. 1c). After 6 days of NGF treatment under oxidative stress, the changes in the characteristics of the CTG-250 cell line were swelling of the cell body and very short stubby processes that failed to elongate into dendrites and axons, whereas the LUC cell line did not show any marked change (Fig. 1c).

To evaluate the extent of those defects in the CTG-250 cell line, cell function was analyzed with LDH and the luciferase assay. Comparison of the luciferase activity of the CTG-250 cell line, which had cells that expressed expanded CTG repeats, with that of repeat-free clone (LUC) cells carrying repeat-free luciferase showed significantly low translation of luciferase, especially with NGF ($P < 0.0001$) (Fig. 4a).

Results of the LDH assay, which reflects the cytotoxicity of cultured cells, appeared to be equivalent to those of the repeat-free cell lines. They did not significantly differ between CTG-250 and LUC cells without NGF

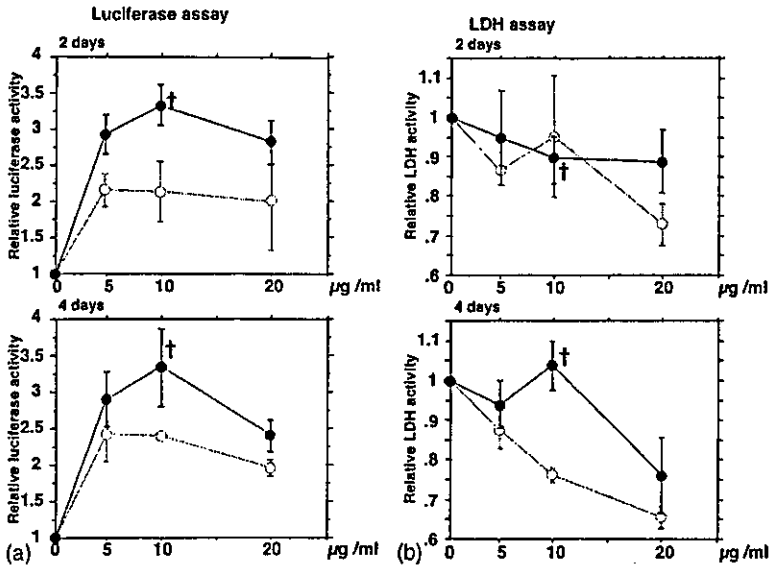

Fig. 8. Inhibition by genistein (isoflavone) of the *cis*-effect (a) and cytotoxicity (b) caused by expanded CTG repeats (data and abbreviations are the same as in Fig. 6).

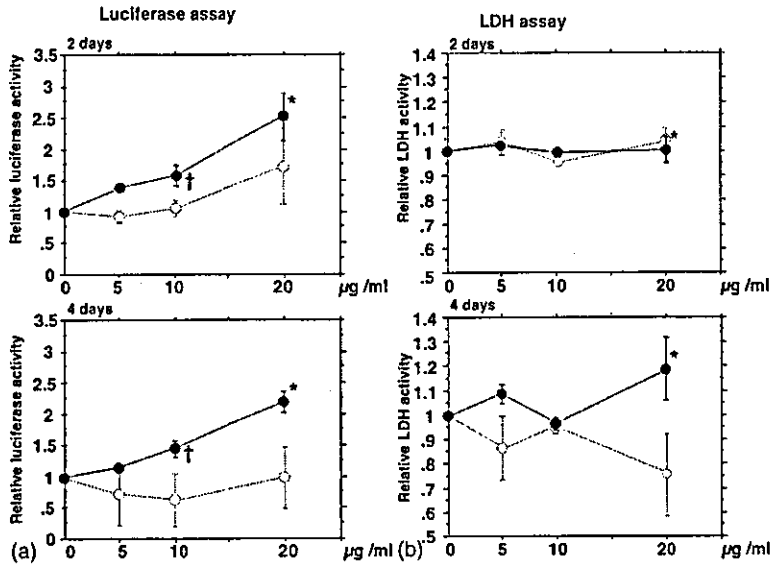

Fig. 9. Inhibition by isosakuranetin (flavanone) of the *cis*-effect (a) and cytotoxicity (b) caused by expanded CTG repeats (data and abbreviations are the same as in Fig. 6).

($P = 0.041$), but with NGF, the difference is significant ($P = 0.0043$) (Fig. 4b). Therefore, expression of the expanded 3′-UTR RNA, affects the NGF-based signaling pathway in particular. These results are evidence that the expression of RNA that carries the 250 CTG repeat expansion in the 3′-UTR region disrupted cell function, especially under oxidative stress. These results also indicate a *cis*-effect on the inhibition of protein production. These findings are consistent with those of a previous report on a muscle cell model [5,35].

3.4. Protective effects of some flavonoids against oxidative stress

When it became clear that the CTG-250 cell to some extent simulates the pathological mechanisms of the neuronal cell of DM1, we screened bioflavonoids and related chemicals for their abilities to inhibit the RNA gain of function seen in this cell system. The structurally related bioflavonoids examined in the third screening are shown in Fig. 5, and their effects on CTG-250 and LUC cell line proliferations are presented in Figs. 6–9. These flavonoids decreased the differences in luciferase activity, cytotoxicity, or both, between the CTG-250 and LUC cell lines. The addition of 5–20 μg/ml or any of them inhibited cell cytotoxicity, lessened the *cis*-effect of CTG repeats, or both. Ononin accelerated luciferase activity that resulted from the reduced *cis*-effect of the CTG repeats (Figs. 6a and 7a, Table 1). Genistein, formononetin and isosakuranetin decreased both the *cis*-effect and cytotoxicity of the CTG repeats significantly (Figs. 8a and b and 9a and b, Tables 1 and 2).

Table 2
Inhibitory effect of flavonoids on different expanded 250 CTG repeats transcribing PC12 neuronal cell lines (CTG250_1, CTG250_2)

Chemical name (MW)	Conc. (μg/μl)	Conc. (μM)	*Cis*-effect		Cytotoxicity	
			CTG250_1	CTG250_12	CTG250_1	CTG250_12
Isoflavone						
Genistein (270)	10	37.0	+	+	+	+
Formononetin (268)	5	18.7	+	+	+	++
	10	37.3	−	−	−	−
Daidzein (254)	10	39.4	−	−	−	−
Flavanone						
Isosakuranetin (286)	10	34.9	+	+	+	+
	20	69.9	+	−	+	−
Coumarin						
Xanthylatin (228)	10	43.9	+	++	+	−
Steroid						
DHEA-S (368)	10	27.2	+	+	+	+

(+) effective for inhibition ($P < 0.05$); (++) highly effective for inhibition ($P < 0.0001$); (−) not effective for inhibition; MW, molecular weight; DHEA-S, dehydroepiandrosterone-sulfate.

Dose–response experiments showed that exposure to ononin (11.6 μM) (Fig. 6, Table 1); formononetin (18.7–37.3 μM) (Fig. 7, Tables 1 and 2); naringenin (73.5 μM) (Table 1); or xanthylatin (43.9–87.7 μM) (Tables 1 and 2) significantly decreased the *cis*-effect of toxic RNA, whereas no decrease in cytotoxicity was found during the 2- to 4-day incubation periods. The use of 10–20 μg/ml of genistein (37.0–74.1 μM) (Fig. 8, Table 1), isosakuranetin (34.9–69.9 μM) (Fig. 9, Table 1), or toringin (48.0 μM) (Table 1), however, progressively decreased not only the *cis*-effect of the expanded CTG repeats but cytotoxicity as well. Interestingly, dehydroepiandrosterone sulfate (DHEA-S) (27.2 μM), which is reported to improve the symptoms of DM1 patients was efficacious against cytotoxicity and the *cis*-effect in our system (Table 1) [33,36].

We have independently constructed two other stable clones containing expanded CTG repeats in the same way (Table 2, CTG250_1, CTG250_12). Using these clones, we confirmed the protective effect of these flavonoid; all of them were revealed to be effective in the same conditions as the previous experiment at a suitable concentration (Table 1). Using these clones, protective effects were also observed with isosakuranetin, formononetin, xanthylatin and DHEA-S, which is almost the same result as that of the CTG-250 and LUC cell lines, except that formononetin showed a protective effect for both *cis*-effect and cytotoxicity (Table 2).

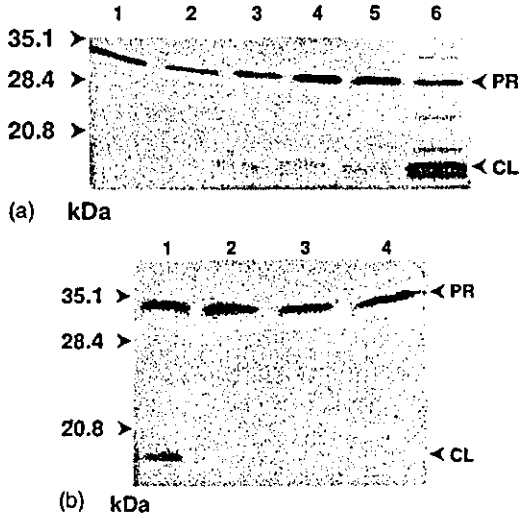

Fig. 10. Oxidative stress increases the active form of caspase-3 (CL) in CTG-250 cells (a), but the increase is inhibited by flavonoid treatment (b). (a) Long incubation of CTG-250 cells in serum-free media with NGF increases cleaved caspase-3 (active form of caspase-3) (CL) more than uncleaved caspase-3 (inactive form) (PR). LUC cells incubated after differentiation (FCS(−), NGF(+)), for 48 h (lane 1), 96 h (lane 2) and 144 h (lane 3), and CTG-250 cells incubated after differentiation (FCS(−), NGF(+)), for 48 h (lane 4), 96 h (lane 5) and 144 h (lane 6). (b) Increase in the active caspase-3 form (CL) in CTG-250 cells is inhibited by flavonoid treatment. Lane 1: no flavonoid, lane 2: ononin (5 μg/ml), lane 3: formononetin (10 μg/ml), lane 4: isosakuranetin (20 μg/ml), PR: inactive form of caspase-3 (procaspase-3), CL: active form of caspase-3 (cleaved caspase-3). Positions to which molecular markers (kDa) migrate are indicated on the left.

3.5. Protective effect of some flavonoids against the cis-effect and cytotoxicity

The underlying cellular mechanisms by which these flavonoids give neuroprotection in this cellular model have yet to be determined, but a significant number of neuronal deaths in a previous C2C12 myoblast cells study done with a transient expression system, showed features of apoptosis with prominent caspase-3 activation [35,37]. We therefore considered whether flavonoid treatment blocks expanded CTG repeat-induced caspase-3 activation in the CTG-250 cell line. First, we used Western blotting to search for formation of the activated form of caspase-3, the p17 form, as well as by cleavage of known caspase-3 substrates [38] and found an increase in the active form of caspase-3 in CTG-250 cells cultured without a flavonoid (Fig. 10a). In cell lysates derived from samples treated at the appropriate concentration with isosakuranetin, genistein, formononetin, or ononin, however, no cleavage of caspase-3 or its substrates was found in the Western blotting (Fig. 10b). Because caspase-3 works during the last stage of apoptotic pathways, it is not clear whether flavonoids directly block this apoptotic cascade, but our findings suggest that inhibition of the *cis*-effect of the CTG repeat expansions also may inhibit apoptotic neuronal death.

4. Discussion

We showed that a PC12 rat neuronal cell line which expresses expanded CTG repeats that carry reporter mRNA can be characterized simply by measuring its gene translational product in order to evaluate the *cis*-effect of expanded CTG repeats. Under oxidative stress, our neuronal cell line underwent neuronal death just after cell differentiation and showed different alternative splicing patterns of the tau gene. Of course, this system is not completely identical to that of the neuronal cells of DM1 patients or the DM1 mouse model because the gene expression pattern of the tau isoforms differs slightly from that of DM1, and no different pattern of abnormal phosphorylation has yet been observed. These differences may be owing to a difference in the species or organs used, the absence of a neuron-glia cell relationship, or the short culture period used in this system. Its simplicity and ease of handling, however, make the system useful for detecting the mechanisms of altered alternative splicing or apoptosis caused by toxic RNA. Further, in this system, although the nuclear membrane disappears at every mitosis before differentiation, it is preserved after the induction of differentiation by NGF. This means the effects of the retention of the expanded CUG repeats carrying mRNA can be determined at any time in detail (Fig. 1a and b). With this

system, we also demonstrated that some flavanones and isoflavones, in particular, isosakuranetin, inhibit the *cis*-effect and cytotoxicity caused by CTG repeat expansions.

Retention of nuclear–cytoplasm transportation is disturbed in cultured DM1 fibroblasts and myoblasts, and increased numbers of probe signals have been confirmed by the FISH method with CUG-repeat or DMPK-specific probes [8,39], resulting in decreased expression of DMPK gene products [40,41]. These phenomena, referred to as the decreased *cis*-effect and reduced cytotoxicity, which are caused by expanded CTG repeats in 3′-UTR may correspond to improvement of the *trans*-effect [5]. The nuclear membrane may have an important role in that situation [13]. Increased luciferase activity in this system, unlike in repeat-free control cells, means that the *cis*-effect of expanded CTG repeats in 3′-UTR was reduced after treatment with several flavonoids. Results of RNA blotting showed that in this system, the amount of gene translation did not differ greatly between CTG-250 and LUC cells. Therefore, the difference in luciferase activity in this system is considered to be a result of translation rather than gene transcription and is generated by repeats that produce RNA intoxication from a disturbance in nucleus-to-cytoplasm transportation in the nuclei [12].

Our findings provide evidence that the expression of expanded 250 CTG repeats in the 3′-UTR region disrupts cellular functions under oxidative stress after differentiation. Quintero-Mora et al. also reported that an expanded 90-CTG repeat in a stable cell line suppressed NGF-induced neuronal differentiation during 6 days of culture [21]. Our system showed not so strong inhibition of NGF-induced neuronal differentiation under oxidative stress, but fragility followed by apoptosis. Because gene expression efficiency differs a bit in every stable cell lines, if the repeat size is beyond the normal range, the repeat size may not necessarily correlate exactly with the toxic effect [42]. So, both 90-CTG repeats carrying a CAT reporter gene and our 250 CTG repeats with a luciferase reporter gene system are suitable for in vitro research on the effects of toxic RNA in the nucleus or tauopathy in the CNS [4,19].

Our findings also indicate that exposure to isosakuranetin, toringin, genistein, or DHEA-S protects and rescues PC12 neuronal cells that transcribe expanded CTG repeats in the 3′-UTR region of the luciferase gene from apoptotic death under the condition of oxidative stress, acting principally via its flavonoid constitution (Table 1). This is the first report of the efficaciousness of flavonoids for ameliorating the RNA gain of function caused by expanded CTG repeats. Flavonoids are reported to have various biological activities and beneficial actions against cancers, coronary heart disease [26], oxidative stress-induced toxicity [43,44,45], and β-amyloid-induced toxicity [46,47], among other pathologies.

Because no chemical ameliorates only cytotoxicity, flavonoids may reduce the *cis*-effect of toxic RNA, causing a reduction in cytotoxicity. Not all the flavonoids examined were equally effective against the *cis*-effect of mRNA and cytotoxicity. The greatest inhibition was produced by isosakuranetin (Fig. 9, Table 1), toringin, genistein, and DHEA-S being less effective (Table 1). Little is known about isosakuranetin, which is present in *Poncirus trifoliata* or *Chromolaena odorata* (Eupolin), and is reported to enhance the proliferation of fibroblasts and endothelial cells [48]. Genistein, a naturally occurring isoflavonoid in soybean, is a well-known anti-carcinogen that is commonly sold as a nutrient. It is reported that the genistein lowers the risk of breast, pancreatic, and prostatic cancers [49–51], although there is a study that did not find it beneficial in vivo [52]. Some steroid derivatives, such as DHEA-S, are reported to be the useful for the improvement of the clinical symptoms of muscular dystrophy [33,36]. The effectiveness of DHEA-S in treating DM1 also was confirmed in our model cell system, as was the usefulness of the system for screening various other chemicals.

A comparison of the chemical structures of isoflavones and flavanone may help us to understand how they inhibit the *cis*-effect and/or cytotoxicity. In the isoflavone group, the only difference between genistein and daidzein is the existence of the hydroxyl group at C-5 (Fig. 5h and k). Replacement of the hydroxyl group at the C-4′ of daidzein with a methoxy group may increase the compound's ability to protect cells (Fig. 5i and k). However, this effect differs slightly in each cell line (CTG-250, CTG250_1 and CTG250_12, Tables 1 and 2). Further, if the phenolic group at C-3 in genistein is moved to C-2, the effect against cytotoxicity is lost (Fig. 5e and h), and if the hydroxyl group at C-4′ in apigenin is replaced with a methyl group (Fig. 5d and e), both effects are lost. In the flavanone group, naringenin possesses a hydroxyl group at the C-5 and C-4′ positions, and it prevents the *cis*-effect only (Fig. 5m). On the other hand, isosakuranetin possesses a hydroxyl group at C-5 and a methyl group at C-4′ (Fig. 5n), and it prevents both the *cis*-effect and cytotoxicity constitutively. Although the only constructive difference among isosakuranetin and acacetin is the existence of a double bond between C-2 and C-3 (Fig. 5d and n), the preventative effect differs greatly.

Based on these findings, the presence of a hydroxyl group either at C-4′ and C-5 in an isoflavone may inhibit cytotoxicity. Similarly, either the hydroxyl group at C-5 or the methyl group at C-4′ in flavanones may inhibit cytotoxicity. It is not known how these flavonoids ameliorate cytotoxicity and the *cis*-effect, but a previous report showed that genistein and daidzein, which are the same natural soybean extract, have the same effect [51]. In our study, genistein was effective, whereas, daidzein was not. These results suggest that the basic flavonoids mechanism against neoplastic and CTG-250 PC12 cells differs in vitro.

Because repeat binding proteins such as CUG-binding protein or muscleblind protein (MBNL1/EXP) are reported to play an important role in nuclear–cytoplasm transporta-

tion and gene expression [11,15,16,18], these flavonoids may intervene in the increment or decrement of the affinity between the repeat-expanded mRNA and repeat-specific binding protein. Likewise, it is not clear whether they will be as effective in the DM1 mouse model and/or treatment of DM1 patients in this PC12-based model cell. Therefore, before starting bioflavonoid treatment, there are various factors that must be clarified by detailed examination: (1) the effectiveness of these flavonoids for DM1 model myoblast cells, (2) the permeability of the blood brain barrier to these flavonoids, and (3) the toxicity of these flavonoids to neuronal and glial cells during long-term culture. Detailed studies with this cell model of the effects of these flavonoids on repeat-mediated toxicity are needed.

In summary, we constructed a neuronal cell model that simulates the pathogenesis of DM1 and discovered that several bioflavonoids ameliorate repeat-mediated *cis*-effects, cytotoxicity, or both, that are produced by expanded CTG repeats. These bioflavonoids may have strong potential as agents against the repeat-mediated *cis*-effect, cytotoxicity or both, caused by expanded CTG DM1 or DM2 repeats. Based on the findings presented, effects mainly are attributable to polyvalent actions of the flavonoid constituents of isosakuranetin, including the ability to modulate apoptotic pathways. The protective/rescuing properties of those flavonoids underlie the potential beneficial effects against gain of function of expanded repeats carrying mRNA and other related pathologies likely to be associated with the deleterious effects of increased production of expanded CUG repeat containing RNA.

Acknowledgements

We thank Dr. M. Miyazono (Department of Neurosurgery, Faculty of Medicine, Kyushu University), Dr. R.W. Shin (Department of Neuropathology, Faculty of Medicine, Tohoku University) and Dr. T. Iwaki (Department of Neuropathology, Faculty of Medicine, Kyushu University) for supplying the rat tau antibody. This study was supported by a Research Grants for Nervous and Mental Disorders (14B-4) from the Ministry of Health, Labor and Welfare of Japan.

References

[1] Harper PS. Myotonic dystrophy, 3rd ed. London: WB Saunders; 2000. p. 17–165.
[2] Fu YH, Pizzuti A, Fenwick Jr RG, King J, Rajnarayan S, Dunne PW, et al. An unstable triplet repeat in a gene related to myotonine muscular dystrophy. Science 1992;255:1256–8.
[3] Fu YH, Friedman DL, Richards S, Pearlman JA, Gibbs RA, Pizzuti A, et al. Decreased expression of myotonin protein kinase mRNA and protein in adult form of myotonic dystrophy. Science 1993; 260:235–8.
[4] Tapscott SJ, Thornton CA. Biomedicine. Reconstructing myotonic dystrophy. Science 2001;293:816–7.
[5] Amack JD, Paguio AP, Mahadevan MS. *Cis* and *trans* effects of the myotonic dystrophy (DM) mutation in a cell culture model. Hum Mol Genet 1999;8:1975–84.
[6] Liquori CL, Ricker K, Moseley ML, Jacobsen JF, Kress W, Naylor SL, et al. Myotonic dystrophy type 2 caused by a CCTG expansion in intron 1 of ZNF9. Science 2001;293:864–7.
[7] Day JW, Ricker K, Jacobsen JF, Rasmussen LJ, Dick KA, Kress W, et al. Myotonic dystrophy type 2: molecular, diagnostic and clinical spectrum. Neurology 2003;60:657–64.
[8] Davis BM, McCurrach ME, Taneja KL, Singer RH, Housman DE. Expansion of a CUG trinucleotide repeat in the 3′ untranslated region of myotonic dystrophy protein kinase transcripts results in nuclear retention of transcripts. Proc Natl Acad Sci USA 1997; 94:7388–93.
[9] Taneja KL. Localization of trinucleotide repeat sequences in myotonic dystrophy cells using a single fluorochrome-labeled RNA probe. Biotechniques 1998;24:472–6.
[10] Timchenko LT. Myotonic dystrophy: the role of RNA CUG triplet repeats. Am J Hum Genet 1999;64:360–4.
[11] Miller JW, Urbinati CR, Teng-umnuay P, Stenberg MG, Byrne SBJ, Thorntonl CA, et al. Recruitment of human muscle blind proteins to $(CUG)_n$ expansions associated with myotonic dystrophy. EMBO 2000;19:4439–48.
[12] Ranum LP, Day JW. Myotonic dystrophy: RNA pathogenesis comes into focus. Am J Hum Genet 2004;74:793–804.
[13] Furuya H, Imai N, Nagano S, Yamada T, Shiokawa K, Kira J. Expression of reporter gene with expanded CTG trinucleotide repeats in 3′-untranslated region using *Xenopus Oocytes*. Ann Neurol 2000;48:441 [abstract].
[14] Timchenko LT, Miller JW, Timchenko NA, DeVore DR, Datar KV, Lin L, et al. Identification of a $(CUG)_n$ triplet repeat RNA-binding protein and its expression in myotonic dystrophy. Nucl Acids Res 1996;24:4407–14.
[15] Takahashi N, Sasagawa N, Suzuki K, Ishiura S. The CUG-binding protein binds specifically to UG dinucleotide repeats in a yeast three-hybrid system. Biochem Biophys Res Commun 2000;277:518–23.
[16] Kino Y, Mori D, Oma Y, Takeshita Y, Sasagawa N, Ishiura S. Muscleblind protein, MBNL1/EXP, binds specifically to CHHG repeats. Hum Mol Genet 2004;13:495–507.
[17] Mankodi A, Logigian E, Callahan L, McClain C, White R, Henderson D, et al. Myotonic dystrophy in transgenic mice expressing an expanded CUG repeat. Science 2000;289:1769–73.
[18] Kanadia RN, Johnstone KA, Mankodi A, Lungu C, Thornton CA, Esson D, et al. A muscleblind knockout model for myotonic dystrophy. Science 2003;302:1978–80.
[19] Sergeant N, Sablonniere B, Schraen-Maschke S, Ghestem A, Maurage CA, Wattez A, et al. Dysregulation of human brain microtubule-associated tau mRNA maturation in myotonic dystrophy type 1. Hum Mol Genet 2001;10:2143–55.
[20] Seznec H, Agbulut O, Sergeant N, Savouret C, Ghestem A, Tabti N, et al. Mice transgenic for the human myotonic dystrophy region with expanded CTG repeats display muscular and brain abnormalities. Hum Mol Genet 2001;10:2717–26.
[21] Quintero-Mora ML, Depardon F, Waring J, Korneluk RG, Cisneros B. Expanded CTG repeats inhibit neuronal differentiation of the PC12 cell line. Biochem Biophys Res Commun 2002;295:289–94.
[22] Biocca S, Cattaneo A, Calissano P. Nerve growth factor inhibits the synthesis of a single-stranded DNA binding protein in pheochromocytoma cells (clone PC12). Proc Natl Acad Sci USA 1984;81:2080–4.
[23] Davis PK, Johnson GV. The microtubule binding of tau and high molecular weight tau in apoptotic PC12 cells is impaired because of altered phosphorylation. J Biol Chem 1999;274:35686–92.
[24] Atabay C, Cagnoli CM, Kharlamov E, Ikomovic MD, Manev H. Removal of serum from primary cultures of cerebellar granule neurons

induces oxidative stress and DNA fragmentation: protection with antioxidants and glutamate receptor antagonists. J Neurosci Res 1996;43:465–75.

[25] Goncharova EI, Nddas A, Rossman TG. Serum deprivation, but not inhibition of growth per se, induces a hypermutable state in Chinese hamster Gl2 cells. Cancer Res 1996;56:752–6.

[26] Marchand LL. Cancer preventive effects of flavonoids: a review. Biomed Pharmacother 2002;56:296–301.

[27] Niwa H, Yamamura K, Miyazaki J. Efficient selection for high-expression transfectants with a novel eukaryotic vector. Gene 1991;108:193–200.

[28] Greene LA, Tischler AS. Establishment of a noradrenergic clonal line of rat adrenal pheochromocytoma cells which respond to nerve growth factor. Proc Natl Acad Sci USA 1976;73:2424–8.

[29] Batistatou A, Greene LA. Aurintricarboxylic acid rescues PC12 cells and sympathetic neurons from cell death caused by nerve growth factor deprivation: correlation with suppression of endonuclease activity. J Cell Biol 1991;115:461–71.

[30] Katoh H, Yasui H, Yamaguchi Y, Aoki J, Fujita H, Mori K, et al. GTPase RhoG is a key regulator for neurite outgrowth in PC12 cells. Mol Cell Biol 2000;20:7378–87.

[31] Anastasiadis PZ, Jiang H, Bezin L, Kuhn DM, Levine RA. Tetrahydrobiopterin enhances apoptotic PC12 cell death following withdrawal of trophic support. J Biol Chem 2001;276:9050–8.

[32] Lowry OH, Rosebrough NJ, Farr AL, Randall RJ. Protein measurement with the Folin phenol reagent. J Biol Chem 1951;193:265–75.

[33] Tsuji K, Furutama D, Tagami M, Ohsawa N. Specific binding and effects of dehydroepiandrosterone sulfate (DHEA-S) on skeletal muscle cells: possible implication for DHEA-S replacement therapy in patients with myotonic dystrophy. Life Sci 1999;65:17–26.

[34] Goedert M, Crowther RA, Garner CC. Molecular characterization of microtubule-associated proteins tau and MAP2. Trends Neurosci 1991;14:193–9.

[35] Usuki F, Takahashi N, Sasagawa N, Ishiura S. Differential signaling pathways following oxidative stress in mutant myotonin protein kinase cDNA-transfected C2C12 cell lines. Biochem Biophys Res Commun 2000;267:739–43.

[36] Sugino M, Ohsawa N, Ito T, Ishida S, Yamasaki H, Kimura F, et al. A pilot study of dehydroepiandrosterone sulfate in myotonic dystrophy. Neurology 1998;51:586–9.

[37] Usuki F, Ishiura S. Expanded CTG repeats in myotonin protein kinase increase susceptibility to oxidative stress. Neuroreport 1998;9:2291–6.

[38] Fujikawa DG, Ke X, Trinidad RB, Shinmei SS, Wu A. Caspase-3 is not activated in seizure-induced neuronal necrosis with internucleosomal DNA cleavage. J Neurochem 2002;83:229–40.

[39] Fardaei M, Rogers MT, Thorpe HM, Larkin K, Hamshere MG, Harper PS, et al. Three proteins, MBNL, MBLL and MBXL, co-localize in vivo with nuclear foci of expanded-repeat transcripts in DM1 and DM2 cells. Hum Mol Genet 2002;11:805–14.

[40] Reddy S, Smith DB, Rich MM, Leferovich JM, Reilly P, Davis BM, et al. Mice lacking the myotonic dystrophy protein kinase develop a late onset progressive myopathy. Nat Genet 1996;3:325–35.

[41] Jansen G, Groenen PJ, Bachner D, Jap PH, Coerwinkel M, Oerlemans F, et al. Abnormal myotonic dystrophy protein kinase levels produce only mild myopathy in mice. Nat Genet 1996;13:316–24.

[42] Furling D, Lam le T, Agbulut O, Butler-Browne GS, Morris GE. Changes in myotonic dystrophy protein kinase levels and muscle development in congenital myotonic dystrophy. Am J Pathol 2003;162:1001–9.

[43] Bastianetto S, Zheng WH, Quirion R. The *Ginkgo biloba* extract (EGb 761) protects and rescues hippocampal cells against nitric oxide-induced toxicity: involvement of its flavonoid constituents and protein kinase C. J Neurochem 2000;74:2268–77.

[44] Sasaki N, Toda T, Kaneko T, Baba N, Matsuo M. Flavonoids suppress the cytotoxicity of linoleic acid hydroperoxide toward PC12 cells. Biol Pharm Bull 2002;25:1093–6.

[45] Sasaki N, Toda T, Kaneko T, Baba N, Matsuo M. Protective effects of flavonoids on the cytotoxicity of linoleic acid hydroperoxide toward rat pheochromocytoma PC12 cells. Chem Biol Interact 2003;145:101–16.

[46] Bastianetto S, Ramassamy C, Dore S, Christen Y, Poirier J, Quirion R. The *Ginkgo biloba* extract (EGb 761) protects hippocampal neurons against cell death induced by β-amyloid. Eur J Neurosci 2000;12:1882–90.

[47] Yao Z, Drieu K, Papadopoulos V. The *Ginkgo biloba extract* EGb 761 rescues the PC12 neuronal cells from β-amyloid-induced cell death by inhibiting the formation of β-amyloid-derived diffusible neurotoxic ligands. Brain Res 2001;889:181–90.

[48] Phan TT, Hughes MA, Cherry GW. Enhanced proliferation of fibroblasts and endothelial cells treated with an extract of the leaves of *Chromolaena odorata* (Eupolin), an herbal remedy for treating wounds. Plast Reconstr Surg 1998;101:756–65.

[49] Knowles LM, Zigrossi DA, Tauber RA, Hightower C, Milner JA. Flavonoids suppress androgen-independent human prostate tumor proliferation. Nutr Cancer 2000;38:116–22.

[50] Dixon RA, Ferreira D. Genistein. Phytochemistry 2002;60:205–11.

[51] Buchler P, Gukovskaya AS, Mouria M, Buchler MC, Buchler MW, Friess H, et al. Prevention of metastatic pancreatic cancer growth in vivo by induction of apoptosis with genistein, a naturally occurring isoflavonoid. Pancreas 2003;26:264–73.

[52] Miltyk W, Craciunescu CN, Fischer L, Jeffcoat RA, Koch MA, Lopaczynski W, et al. Lack of significant genotoxicity of purified soy isoflavones (genistein, daidzein, and glycitein) in 20 patients with prostate cancer. Am J Clin Nutr 2003;77:875–82.

Article

Involvement of caspase-4 in endoplasmic reticulum stress-induced apoptosis and Aβ-induced cell death

Junichi Hitomi,[1,6] Taiichi Katayama,[1,6] Yutaka Eguchi,[2,6,7] Takashi Kudo,[3] Manabu Taniguchi,[1,6] Yoshihisa Koyama,[1,6] Takayuki Manabe,[1,6] Satoru Yamagishi,[1,6] Yoshio Bando,[4] Kazunori Imaizumi,[5] Yoshihide Tsujimoto,[2,6,7] and Masaya Tohyama[1,6]

[1]Department of Anatomy and Neuroscience, [2]Division of Molecular Genetics, and [3]Division of Psychiatry and Behavioural Proteomics, Department of Post-Genomics and Diseases, Graduate School of Medicine, Osaka University, Suita, Osaka 565-0871, Japan
[4]Department of Anatomy, Asahikawa Medical College, Midorigaoka Higashi, Asahikawa, Hokkaido, 078-8510, Japan
[5]Division of Structural Cell Biology, Nara Institute of Science and Technology, Takayama, Ikoma, Nara 630-0101, Japan
[6]21st Century COE Program, Japan Society for the Promotion of Science, Chiyoda-ku, Tokyo 102-8471, Japan
[7]Solution Oriented Research for Science and Technology of Japan, Science and Technology Agency, Honcho 4-1-8, Kawaguchi, Saitama, 332-0012, Japan

Recent studies have suggested that neuronal death in Alzheimer's disease or ischemia could arise from dysfunction of the endoplasmic reticulum (ER). Although caspase-12 has been implicated in ER stress-induced apoptosis and amyloid-β (Aβ)–induced apoptosis in rodents, it is controversial whether similar mechanisms operate in humans. We found that human caspase-4, a member of caspase-1 subfamily that includes caspase-12, is localized to the ER membrane, and is cleaved when cells are treated with ER stress-inducing reagents, but not with other apoptotic reagents. Cleavage of caspase-4 is not affected by overexpression of Bcl-2, which prevents signal transduction on the mitochondria, suggesting that caspase-4 is primarily activated in ER stress-induced apoptosis. Furthermore, a reduction of caspase-4 expression by small interfering RNA decreases ER stress-induced apoptosis in some cell lines, but not other ER stress-independent apoptosis. Caspase-4 is also cleaved by administration of Aβ, and Aβ-induced apoptosis is reduced by small interfering RNAs to caspase-4. Thus, caspase-4 can function as an ER stress-specific caspase in humans, and may be involved in pathogenesis of Alzheimer's disease.

Introduction

Recently, it has been reported that some human diseases, such as Alzheimer's disease (AD), Parkinson's diseases, and cystic fibrosis, and neuronal damage by ischemia are related to stress acting on the ER, which leads to intraluminal accumulation of unfolded proteins (Katayama et al., 1999; Wigley et al., 1999; Imai et al., 2000, 2001; Nakagawa et al., 2000; Sato et al., 2001; Tamatani et al., 2001). Stress on the ER can be induced in vitro by depletion of calcium from the ER lumen, inhibition of asparagine N-linked glycosylation, reduction of disulfide bonds, expression of mutant proteins, and ischemia (Imaizumi et al., 2001). ER stress induces three major cellular responses: unfolded protein response (UPR), ER-associated degradation, and apoptosis. Cells exposed to ER stress can up-regulate genes encoding chaperones that facilitate the protein folding process in the ER and reduce overall translation (UPR; Harding et al., 1999; Kaufman, 2002; Forman et al., 2003), or enhance proteasomal degradation of misfolded ER protein in cytosol (Bonifacino and Weissman, 1998; Travers et al., 2000), to reduce the accumulation and aggregation of misfolded proteins, and relieve cells from the stress (Kozutsumi et al., 1988). On the other hand, excessive or long-termed ER stress results in apoptotic cell death, involving nuclear fragmentation,

Address correspondence to Taiichi Katayama, Dept. of Anatomy and Neuroscience, Graduate School of Medicine, Osaka University, Suita, Osaka 565-0871, Japan. Tel.: 81-6-6879-3221. Fax: 81-6-6879-3229. email: katayama@anat2.med.osaka-u.ac.jp; or Yutaka Eguchi, Division of Molecular Genetics, Dept. of Post-Genomics and Disease, Graduate School of Medicine, Osaka University, Suita, Osaka 565-0871, Japan. Tel.: 81-6-6879-3363. Fax: 81-6-6879-3369.
email: eguchi@gene.med.osaka-u.ac.jp

Key words: apoptosis; ER stress; caspase-4; Alzheimer's disease; amyloid-β

Abbreviations used in this paper: Aβ, amyloid-β; AD, Alzheimer's disease; ICE, interleukin-1β converting enzyme; RNAi, RNA interference; siRNA, small interfering RNA; TRAF2, tumor necrosis factor receptor-associated factor 2; UPR, unfolded protein response.

The Journal of Cell Biology, Volume 165, Number 3, May 10, 2004 347–356
http://www.jcb.org/cgi/doi/10.1083/jcb.200310015

condensation of chromatin, and shrinkage of the cell body (Imaizumi et al., 2001). Several mechanisms that activate apoptotic signaling pathways have been reported. For example, the UPR increases the transcription of CHOP/GADD153 (Brewer et al., 1997), which is closely associated with cell death (Zinszner et al., 1998), recruitment of tumor necrosis factor receptor–associated factor 2 (TRAF2) to activated IRE1α induces c-Jun NH_2-terminal kinase activation (Urano et al., 2000), or calpain activates downstream caspase cascade (Nakagawa and Yuan, 2000). However, little is known about the precise mechanisms to lead to ER stress-induced cell death in humans.

Activation of caspases, a family of cysteine proteases that cleave substrates at specific aspartate residues, is a central mechanism in the apoptotic cell death process (Salvesen and Dixit, 1997; Thornberry and Lazebnik, 1998). Most of apoptosis-inducing stimuli lead to release of cytochrome *c* from mitochondria, which binds to Apaf-1 to activate caspase-9 (Li et al., 1997; Zou et al., 1997), one of initiator caspases with a long pro-domain, and then the activated caspase-9 cleaves effector caspases (Li et al., 1997), including caspases 3 and 7 with a relatively short pro-domain, to activate them. Antiapoptotic Bcl-2 family proteins can rescue cells from apoptosis by protecting mitochondria to prevent cytochrome *c* release (Kluck et al., 1997; Yang et al., 1997). Several initiator caspases are known to be activated upstream of the mitochondrial dysfunction by specific apoptotic stimuli. For example, Fas stimulation can activate caspase-8 (Fernandes-Alnemri et al., 1996; Muzio et al., 1996), which cannot be inhibited by Bcl-2 (Scaffidi et al., 1998). Among 14 known caspases, caspase-12 seems to be involved in signaling pathways specific to ER stress-induced apoptosis (Nakagawa et al., 2000). Pro–caspase-12 is predominantly localized to the ER, and is specifically cleaved by ER stress. Furthermore, caspase-12–deficient mice show a reduced sensitivity to amyloid-β (Aβ), which is found in brains from Alzheimer's patients (Selkoe, 1986) and shown to cause neuronal cytotoxicity (Yankner et al., 1989). Based on these findings, caspase-12 has been suggested to play an important role in the pathogenesis of AD and to represent a potential target of treatment. However, caspase-12 has only been cloned in the mouse and rat so far, and therefore it is controversial whether similar mechanisms operate in humans (Katayama et al., 1999; Rao et al., 2001; Fischer et al., 2002).

Human genome sequence that is highly homologous to mouse caspase-12 has been identified at the locus within the caspase-1/interleukin-1β converting enzyme (ICE) genes cluster on chromosome 11q22.3 (Fischer et al., 2002), but the gene is interrupted by frame shift and premature stop codon, and also has amino acid substitution in the critical site for caspase activity (Fischer et al., 2002). Therefore, human caspase-12 seems to be lost, and the caspases that substitute for caspase-12 to be activated specifically by ER stress have not been identified in humans so far. We described here that human caspase-4 located within the caspase-1/ICE genes cluster shows similar characteristics to mouse caspase-12. The role of the caspase-4 in ER stress-induced apoptosis and Aβ-induced cell death will be discussed.

Results

Identification of caspase-4 as a gene homologous to caspase-12

To detect a caspase that was specifically involved in ER stress, we screened human colon cDNA libraries by the plaque hybridization method using the mouse caspase-12 gene as a probe. Human caspase-4 was cloned as the most homologous gene to mouse caspase-12, in agreement with the fact that both molecules belong to the caspase-1/ICE subfamily within the caspase family (Kamens et al., 1995; Lin et al., 2000). Although caspase-5, which has slightly less homology to caspase-12 (caspase-4: 48%; caspase-5: 45%), was also isolated, the screening process yielded much more caspase-4 clones than caspase-5. Because caspase-4 but not caspase-5 was expressed in the cell lines used in this work, which underwent apoptosis in response to ER stress, we assumed that human caspase-4 might functionally substitute for mouse caspase-12 in the human system, and further analyzed the possible role of caspase-4 as a mediator of ER stress-induced apoptosis.

Subcellular localization of caspase-4

First, we studied the subcellular localization of endogenous caspase-4 in SK-N-SH human neuroblastoma cells. Immunofluorescence microscopy showed that immunostaining pattern of caspase-4 strictly overlapped with that of ER markers such as GRP78 and GRP94 (Fig. 1, a–c). Immunoreactivity of caspase-4 was found to overlap only in part with fluorescence signals from Mitotracker (Fig. 1, d–f). These results suggest that caspase-4 was localized predominantly to the ER, and to the mitochondria in addition. The similar results were obtained using HeLa cells (Fig. 1, g–l). When caspase-4 fused with GFP at its COOH terminus was overexpressed in HeLa cells to see the subcellular localization in live cells, most of the fluorescent signals from caspase-4/GFP fusion protein overlapped with those from ER-tracker (Fig. 1, m–o), confirming predominant localization of caspase-4 to the ER by non-immunological method. The immunoelectron microscopic analysis showed that the immunoreactive signals for caspase-4 were found on the ER and mitochondria (Fig. 1, p–r), but much less signals on the nuclei (Fig. 1 r). We also performed biochemical fractionation analysis. Although we could not eliminate contamination of ER marker proteins in the mitochondria-enriched fraction using SK-N-SH cells, probably because we could not disrupt cells homogeneously as the cell line displays heterogeneity in cellular morphology, microsome-enriched fraction does not seem to contain mitochondria and cytosol (Fig. 1 s). Under these conditions, caspase-4 was recovered in both mitochondria-enriched fraction and microsome-enriched fraction, and in cytosolic fraction to a lesser extent (Fig. 1 s), indicating that caspase-4 was surely in microsome-enriched fraction. From these results, we concluded that caspase-4 was localized to the ER, and to the mitochondria in addition, in both SK-N-SH and HeLa cells.

Specific cleavage of caspase-4 by ER stress and Aβ treatments

To examine whether caspase-4 was specifically cleaved by ER stress, we analyzed the cleavage of pro–caspase-4 in re-

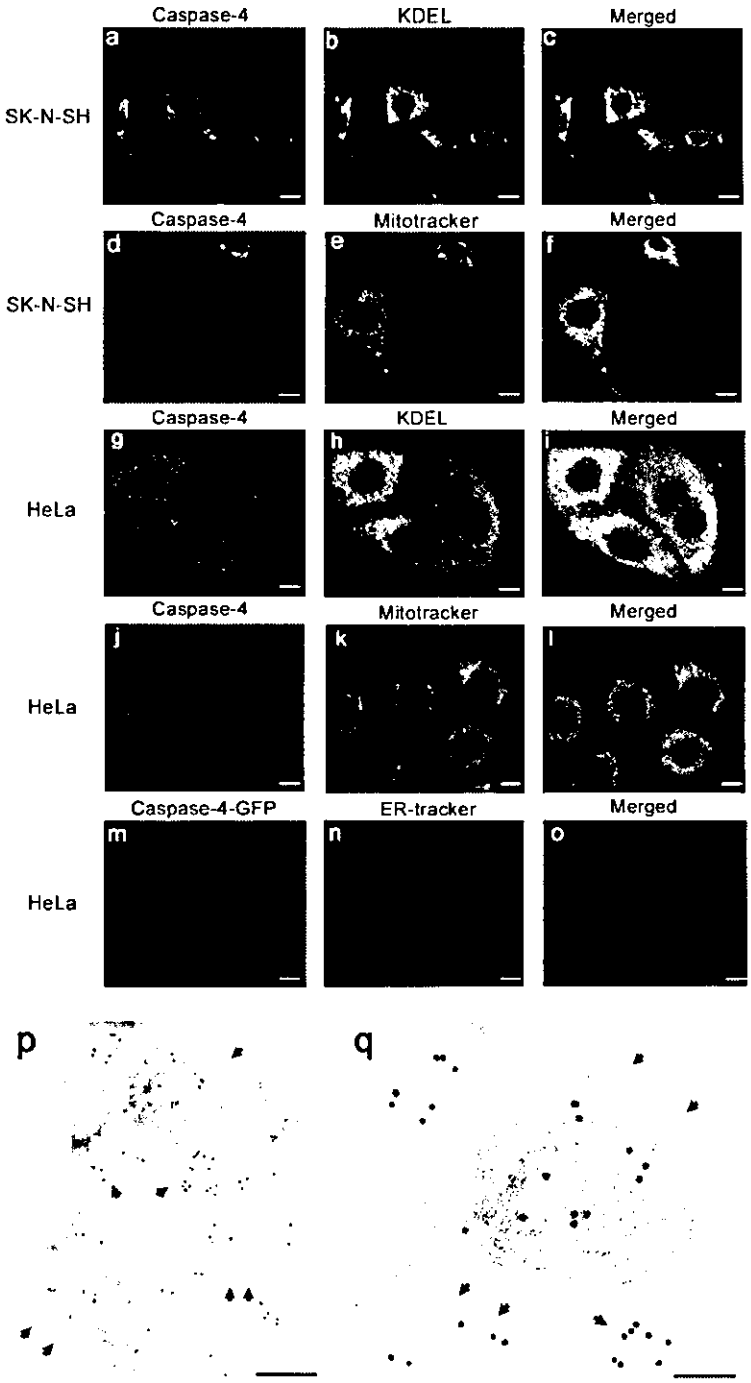

r

	Nuclear	Mitochondria	ER	Cytosol	total
Gold	0	359	392	169	920
%	0	39	43	18	100

s

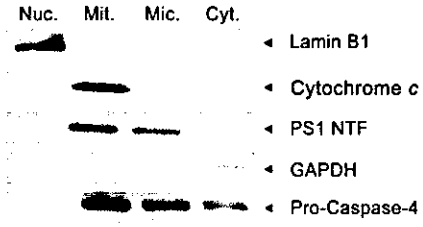

Figure 1. **Localization of caspase-4 in SK-N-SH and HeLa cells.** (a–l) SK-N-SH cells (a–f) or HeLa cells (g–l) were stained with anti–caspase-4 and anti-KDEL antibodies (a and g, caspase-4, green; b and h, KDEL, red; c and i, overlapping, yellow), or with anti–caspase-4 antibody and Mitotracker (d and j, caspase-4, green; e and k, Mitotracker, red; f and l, overlapping, yellow), and observed under a confocal microscope as described in Materials and methods. Anti-KDEL antibody detects both GRP78 and GRP94 (ER markers), whereas Mitotracker stains the mitochondria. (m–o) HeLa cells were transfected with a caspase-4–GFP fusion gene, and were stained with ER-tracker (m, caspase-4, green; n, ER-tracker, blue; o, overlapping, blue-green), and observed under a nonconfocal fluorescence microscope. Bars, 5 μm. (p and q) Immunoelectron microscopic analysis was performed for SK-N-SH cells as described in Materials and methods. Photograph shown in panel q is the enlarged image of a part of photograph p. Gold grains showed the immunoreactivity of caspase-4, and blue and red arrows showed the ER and mitochondria, respectively. Bars: (p) 200 nm; (q) 90 nm. (r) Gold grains observed on indicated organelles in immunoelectron microscopic analysis were counted and displayed. (s) Biochemical fractionation was performed as described in Materials and methods, and analyzed by Western blotting using the indicated antibodies. Lamin B1, nuclear marker; cytochrome *c*, mitochondrial marker; presenilin-1 NH_2-terminal fragment (PS1 NTF), microsomal marker; and glyceraldehyde-3-phosphate dehydrogenase (GAPDH), cytosolic marker.

sponse to several apoptotic stimuli (Fig. 2 a). We found that cleavage of pro–caspase-4 was induced in SK-N-SH cells by treatment with tunicamycin and thapsigargin, both of which caused ER stress. In contrast, when cells were exposed to non-ER stress inducers such as etoposide, staurosporine, and UV at a dose providing similar extent of cell death to that by tunicamycin and thapsigargin, final cleavage products of pro–caspase-4 (Fig. 2 a, cleaved-caspase-4, arrowhead) was not observed. Although the bands shown by the asterisks in Fig. 2 a, which should be derived from pro–caspase-4 by unknown processing reaction, judging from the data below (Fig. 4 b), were also increased, they were also observed in nontreated cells, so we speculated that the bands were not the final processed form of caspase-4. Under the same conditions, cleavage of caspases 3 and 7, the downstream caspases, was observed regardless of apoptotic stimulations (Fig. 2 a). These results suggest that caspase-4 is specifically activated by apoptotic stimuli inducing ER stress, but not by other stimuli that do not cause ER stress.

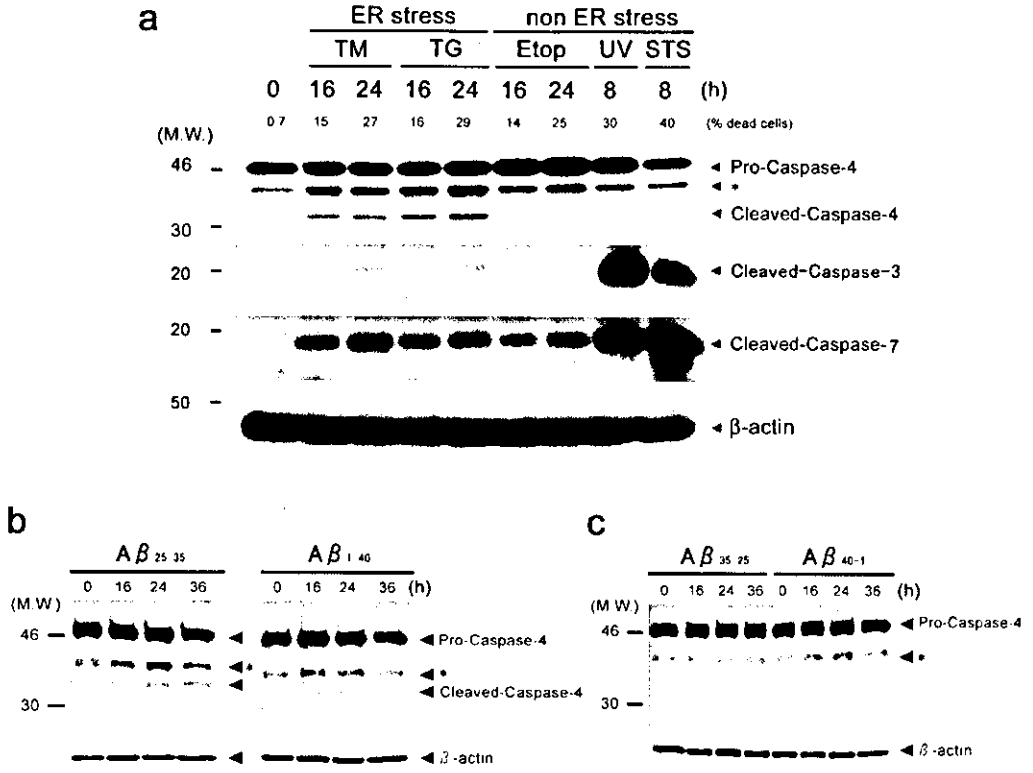

Figure 2. **Specific cleavage of caspase-4 by ER stress and Aβ treatment.** (a) SK-N-SH cells were treated with 1 μg/ml tunicamycin (TM), 0.5 μM thapsigargin (TG), 100 μM etoposide (Etop), or 0.1 μM staurosporine (STS) for indicated periods, or irradiated with 150 J/m^2 UV followed by incubation for indicated periods. Equal amounts of cell lysates (15 μg) were analyzed by Western blotting using anti–caspase-4 antibody (top), anti–caspase-3 antibody (second from top), anti–caspase-7 antibody (third from top), or anti–β-actin antibody (bottom). Positions of pro–caspase-4, cleaved caspase-4, cleaved caspase-3, cleaved caspase-7, and β-actin are indicated. Extent of cell death assessed by MTS assay after incubation for indicated periods are also shown at the top of the gels. (b) SK-N-SH cells were treated with 25 μM synthetic $A\beta_{25-35}$ or 5 μM $A\beta_{1-40}$ peptides for the indicated periods. Equal amounts of cell lysates (15 μg) were analyzed by Western blotting using anti–caspase-4 antibody (top) and anti–β-actin antibody (bottom) as a control. Positions of pro–caspase-4, cleaved caspase-4, and β-actin are indicated. (c) SK-N-SH cells were treated with the reverse peptides (25 μM $A\beta_{35-25}$ and 5 μM $A\beta_{40-1}$, respectively) for the indicated periods, and cleavage of caspase-4 was examined as in panel b. (a–c) Bands marked by asterisks are likely to be derived from pro–caspase-4 by unknown processing reaction.

To address the possibility that caspase-4 contributes to the mechanism of Aβ-induced cell death in humans, we examined the cleavage of caspase-4 in SK-N-SH cells after treatment with Aβ. When cells were incubated with 25 μM $A\beta_{25-35}$ or 5 μM $A\beta_{1-40}$, cleavage of caspase-4 was observed (Fig. 2 b). In contrast, treatment of cells with the reverse peptides ($A\beta_{35-25}$ and $A\beta_{40-1}$, respectively), which were not toxic, did not induce the cleavage of caspase-4 (Fig. 2 c). These results suggest that caspase-4 is activated by neurotoxic Aβ treatment similar to ER stress-induced apoptosis.

Cleavage of caspase-4 in the presence of Bcl-2

To confirm that cleavage of caspase-4 was not due to other caspases activated downstream of the mitochondrial pathway, we examined the effect of overexpression of Bcl-2 and Bcl-x_L on apoptosis induced by tunicamycin. Apoptotic nuclear morphological changes were induced by treatment of vector transfectants of SK-N-SH and of HeLa cells with tunicamycin for 30 h, but such changes were completely suppressed by overexpression of Bcl-2 (Fig. 3) or Bcl-x_L (not depicted), indicating that the apoptotic signaling pathway downstream of mitochondria was not operating in cells with overexpression of these antiapoptotic proteins. However, cleavage of caspase-4 after 16 h of tunicamycin treatment was only slightly affected by overexpression of Bcl-2 (Fig. 3) or Bcl-x_L (not depicted). These results suggested that caspase-4 is largely activated before the activation of effector caspases during ER stress-induced cell death.

Requirement of caspase-4 for ER stress- and Aβ-induced apoptosis

To determine whether caspase-4 is required for ER stress-induced cell death, SK-N-SH cells that expressed endogenous caspase-4 were transfected with small interfering RNA (siRNA) to caspase-4 or GFP as a control. Immunofluorescence analysis showed that the amount of caspase-4 was substantially decreased by incubation for 60 h after transfection with siRNA directed against caspase-4, but immunoreactivity of caspase-4 was not affected by transfection with GFP-siRNA, when compared with nontransfected cells (Fig. 4 a). Western blot analysis also showed that the amount of caspase-4 was decreased by siRNA to caspase-4 (Fig. 4 b). These re-

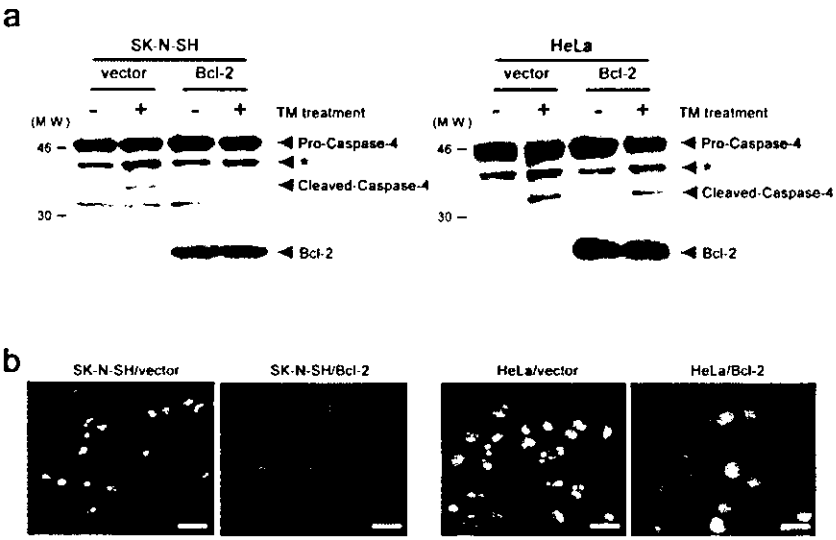

Figure 3. **No effect of Bcl-2 overexpression on ER stress-induced cleavage of caspase-4.** (a) SK-N-SH cells (left) and HeLa cells (right) stably transfected with the vector or a Bcl-2 expression system were incubated with (+) or without (−) 1 μg/ml tunicamycin for 16 h. Equal amounts of cell lysates were analyzed by Western blotting using anti–caspase-4 antibody (top) and anti–Bcl-2 antibody (bottom). Positions of pro–caspase-4, cleaved caspase-4, and Bcl-2 are indicated. Asterisks show processed caspase-4 as described in Fig. 2 a. (b) The indicated cells were treated with 1 μg/ml tunicamycin for 30 h, stained with Hoechst 33342, and observed under a fluorescence microscope. Bars, 25 μm.

sults showed that the siRNA could diminish the amount of caspase-4, and that the antibody used here specifically recognized caspase-4 in immunohistochemical analysis.

We next examined the effect of decrease in caspase-4 level by siRNA on ER stress-induced apoptosis. Assessment of cell death on the basis of morphological changes showed that ~60% of untransfected SK-N-SH cells were killed by treatment with thapsigargin for 40 h. The extent of cell death was unaffected by transfection with siRNA to GFP (Fig. 4 c). In contrast, only ~30% of the cells died after being transfected with caspase-4 siRNA and exposed to the same stimulation with thapsigargin (Fig. 4 c). As shown in Fig. 4 b, treatment with thapsigargin for 24 h yielded lower level of cleaved-caspase-4 in the cells transfected with caspase-4 siRNA than in the cells transfected with GFP-siRNA. Because the amount of cleaved caspase-4 shown in Fig. 4 b seemed to correlate with the extent of cell death in Fig. 4 c, incomplete inhibition of cell death by transfection with caspase-4 siRNA could be due to residual activity of caspase-4. These results indicate that cells with decreased expression of caspase-4 become more resistant to ER stress-induced cell death.

When cell death was examined by the MTS assay, treatment with caspase-4 siRNA, but not with GFP-siRNA, increased the resistance to ER stress-induced cell death (Fig. 4 d). The increase in the resistance to ER stress-induced cell death was also observed when siRNA to caspase-4 with a different sequence (caspase-4 siRNA-b) was used (Fig. 4 d), indicating that the effect was due to the decreased expression of caspase-4, but not by a specific side effect of caspase-4 siRNA that might affect the expression of other genes. On the other hand, the efficiency of cell death induced by etoposide treatment was not significantly affected by both caspase-4 siRNAs (Fig. 4 d). Therefore, caspase-4 is likely to be specifically involved in ER stress-induced cell death.

To know whether caspase-4 is involved in ER stress-induced cell death in other cell lines, we examined the effect of caspase-4 siRNA using HeLa cells. As shown in Fig. 4 e, treatment of HeLa cells with caspase-4 siRNA significantly increased the resistance to ER stress-induced cell death, although the extent of the increase in resistance was less than that observed for SK-N-SH cells. This is probably because some other apoptotic mechanisms might also operate simultaneously in HeLa cells. Therefore, we concluded that caspase-4 is likely to be involved in ER stress-induced cell death at least in part in HeLa cells.

We next examined whether caspase-4 is involved in Aβ-induced cell death. When treated with $A\beta_{25-35}$, SK-N-SH cells transfected with caspase-4 siRNA showed significant reduction in cell death compared with the cells transfected with GFP-siRNA (Fig. 4 f). From these results presented here, we concluded that caspase-4 is involved in Aβ-induced cell death, as well as in ER stress-induced cell death.

Discussion

It has been known that apoptotic morphological changes are observed in cell death caused by ER stress (Imaizumi et al., 2001). Caspases are activated to transmit apoptotic signals transcending the difference in species (Alnemri et al., 1996). In rodents, caspase-12 mediates apoptosis specifically in response to ER stress (Nakagawa et al., 2000). Although human caspase-12 gene is transcribed into mRNA, mature caspase-12 protein would not be produced, because the gene is interrupted by frame shift and premature stop codon (Fischer et al., 2002). Furthermore, it contains amino acid substitution in the critical site, which leads to loss of function in several caspases (Fischer et al., 2002). Thus, human caspase-12 does not seem to function in ER stress-induced apoptosis, and some other caspases with similar structure might substitute functionally for caspase-12 in humans. The caspase-12 gene is located within a region where caspase-1/ICE subfamily genes cluster (caspases 1, 4, 5, 12 in human and caspases 1, 11, 12 in mouse). No locus with a comparably high homology to rodent caspase-12 could be found in the human genome. Caspases 4 and 5 are located between caspases 1 and 12 in human genome, whereas only caspase-11 is located between caspases 1 and 12 in mouse. Although it is not known why the region in human genome contains gene duplication, caspases 4 and 5 have been thought to function similarly to caspases 11 and 12. Mouse caspase-11

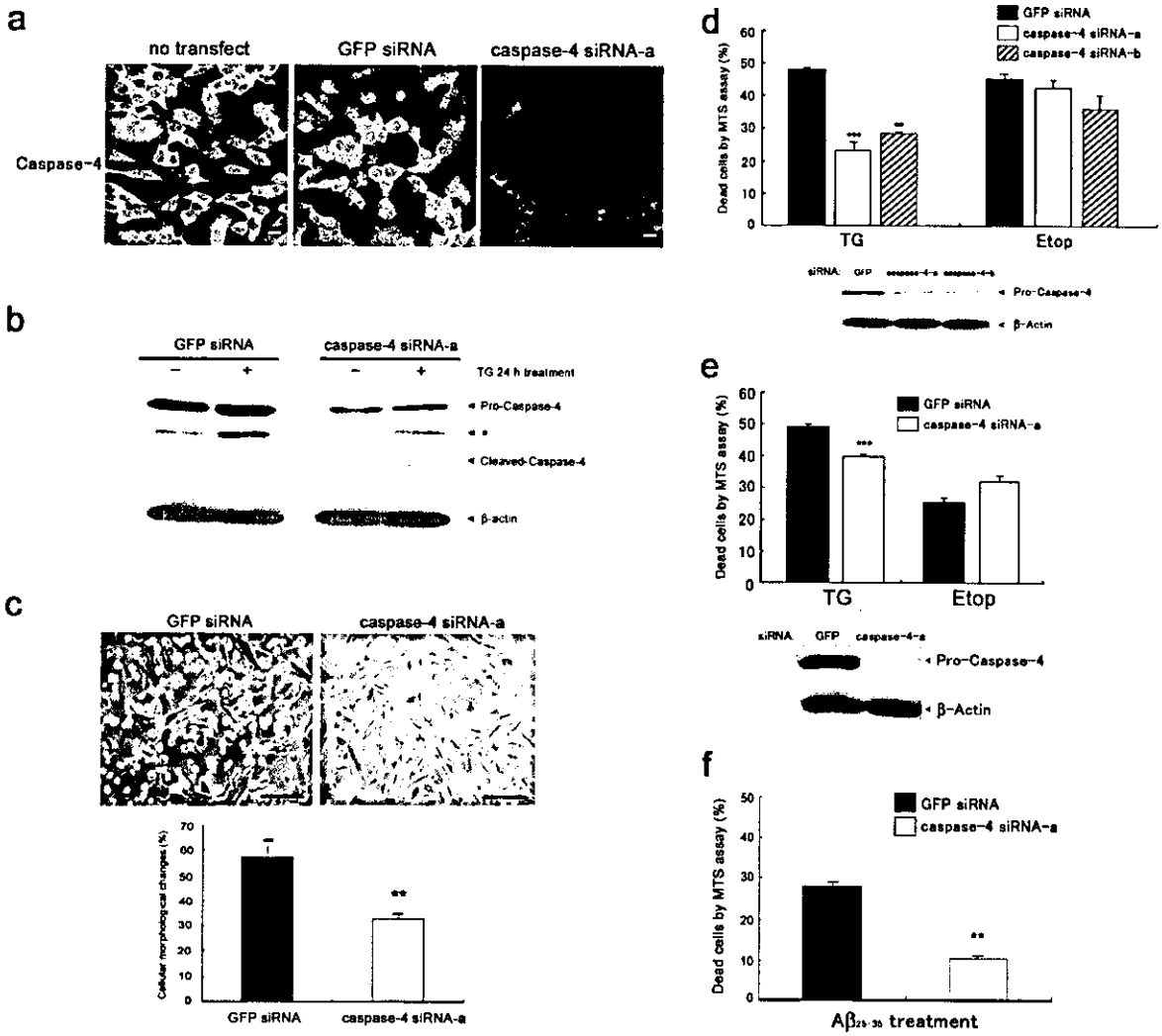

Figure 4. **Decrease in ER stress- or Aβ-induced cell death after siRNA-mediated reduction of caspase-4 expression.** (a) SK-N-SH cells were transfected with siRNA oligos (1 μg oligo/24 well plate) to GFP (control) or caspase-4 (siRNA-a). After incubation for 60 h, cells were fixed and stained with caspase-4 antibodies as described in Materials and methods. Bars, 5 μm. (b) Cells were transfected as in panel a. After incubation for 60 h, cells were incubated with (+) or without (−) 0.5 μM thapsigargin for 24 h. Equal amounts of cell lysates (10 μg) were analyzed by Western blotting using anti–caspase-4 antibody (top) or anti–β-actin antibody (bottom). (c) Top panels show representative phase-contrast images of GFP siRNA-transfected cells (left) and caspase-4 siRNA-a–transfected cells (right) after treatment with 0.5 μM thapsigargin for 40 h. The bottom panel shows the extent of cell death assessed by morphological changes, and expressed as the mean ± SEM for three independent experiments as described in Materials and methods. Asterisks show a significant difference from controls (GFP siRNA-transfected cells): **, indicates $P < 0.01$. Bars, 50 μm. (d) Cells were transfected with the indicated siRNAs, and cell viability after 0.5 μM thapsigargin or 100 μM etoposide treatment for 40 h was estimated by the MTS assay. Results were expressed as the mean ± SEM for three independent experiments. Asterisks show a significant difference from controls: **, indicates $P < 0.01$; ***, indicates $P < 0.001$. Bottom panel shows reduction of caspase-4 level by the indicated siRNAs assessed by Western blotting as described in panel b. (e) HeLa cells were transfected with GFP siRNA or caspase-4 siRNA-a as described in Materials and methods. After incubation for 24 h, cells were incubated with 0.5 μM thapsigargin for 40 h, and then viability was estimated as described in panel d. Each value represents the mean ± SEM for three independent experiments. Asterisks show a significant difference from controls: ***, indicates $P < 0.001$. (f) SK-N-SH cells were transfected with GFP siRNA or caspase-4 siRNA-a. After incubation for 60 h, cells were incubated with 25 μM $A\beta_{25-35}$ peptide for 40 h, and then viability was estimated as described in panel d. Each value represents the mean ± SEM for three independent experiments. Asterisks show a significant difference from controls: **, indicates $P < 0.01$.

is essential for the activation of caspase-1/ICE to promote pro–IL-1β (interleukin-1β) processing (Wang et al., 1996, 1998). On the other hand, caspase-5 is likely involved in processing of pro–IL-1β together with caspase-1/ICE (Martinon et al., 2002) and the caspase-5 gene resembles the mouse caspase-11 in its lipopolysaccharide inducibility (Lin et al., 2000). Therefore, caspase-5 should be the orthologue of caspase-11. Here, the screening process yielded the caspase-4 gene as the homologous gene to mouse caspase-12. Thus, caspase-4 is the best candidate that would function similarly to mouse caspase-12 in ER stress-induced cell death in humans.